MSUCL-196
COO-1779-87
LBL-3441
09/1979

THE DECAY OF ^{201}Pb

R. E. Doebler* and Wm. C. McHarris

Department of Chemistry,† Cyclotron Laboratory,‡

and Department of Physics

and

W. H. Kelly

Cyclotron Laboratory‡ and Department of Physics

Michigan State University

East Lansing, Michigan 48824

*Address while much of this paper was being written: Lawrence Berkeley Laboratory, Berkeley, California. Present address: General Electric Co., San Jose, California.

†Supported in part by the U.S. Energy Research and Development Administration.

‡Supported in part by the U.S. National Science Foundation.

Abstract:

γ rays emitted in the decay of 9.4-h ^{201}Pb were studied with Ge(Li) and NaI(Tl) detectors in singles, anti-Compton, anticoincidence, and integral coincidence configurations. The construction of a consistent decay scheme including 66 of the 74 γ rays observed in the decay of ^{201}Pb was also aided by a two-dimensional γ-γ coincidence experiment of 4096 × 4096 channels using two Ge(Li) detectors. The proposed levels in ^{201}Tl lie at 0, 331.15, 692.40, 1098.4, 1134.8, 1157.4, 1238.8, 1277.1, 1290.0, 1330.4, 1401.2, 1420.0, 1445.8, 1479.9, 1575.1, 1617.4, 1639.5, 1672.0, and 1755.3 keV with possible additional levels at 1550.5 and 1712.5 keV. Using existing conversion-electron data, conversion coefficients were calculated and multipolarity assignments proposed for 25 transitions. Based on these multipolarities, photon branching ratios, and logft values, unique spin and parity assignments have been made for several states and limits placed on others. The resulting decay scheme is compared with recent theoretical calculations of level energies and γ transition probabilities, using the intermediate-coupling unified model.

[RADIOACTIVITY ^{201}Pb [from ^{203}Tl(p,3n) and ^{203}Tl(^{3}He,5n)^{201}Bi $\xrightarrow{\varepsilon}$ ^{201}Pb]; measured E_γ, I_γ, α_K, α_L; deduced logft; ^{201}Tl deduced levels, J, π; Ge(Li) singles and γ-γ coinc.]

I. INTRODUCTION

The neutron-deficient odd-mass Tl isotopes have been the subject of numerous theoretical investigations, the most recent being those of Covello and Sartoris,[1] Alaga and Ialongo,[2] and Azziz and Covello.[3] These recent calculations have been made using the intermediate-coupling unified model in which collective effects, treated as vibrations of the spherical core, are coupled more or less strongly to the single-particle states. Because the odd-mass Tl isotopes are only one proton removed from the Z=82 closed shell and only a few neutrons from the N=126 closed shell, they are an ideal choice for calculations using this model.

Since the level schemes of ^{207}Tl, ^{205}Tl, and ^{203}Tl obtained from radioactive decay are relatively simple and have been studied thoroughly, we have started our investigation of these isotopes with the states in ^{201}Tl populated by the decay of 9.4-h ^{201}Pb. In a forthcoming paper[4] we will present a study of states in ^{199}Tl populated by 90-min ^{199}Pb.

^{201}Pb was first reported in 1946 by Howland, Templeton, and Perlman[5] as a 5-h activity resulting from the reaction, ^{203}Tl(d,4n)^{201}Pb. In 1950 Neuman and Perlman[6] reported an 8±2-h Pb activity as the daughter of both the 62 min and 2-h isomers of ^{201}Bi. In the following years the decay of ^{201}Pb was studied by numerous groups[7-11] using magnetic β-ray spectrometers for internal-conversion electron measurements and NaI(Tl) detectors for photons. The most recent and comprehensive of these studies was published by Aasa

et al.[12] in 1964. Using an iron-yoke double-focusing β spectrometer, they assigned 32 γ transitions to the decay of ^{201}Pb and proposed a decay scheme containing 10 excited levels. However, their decay scheme was far from complete and contained many uncertainties, which prompted the present investigation.

II. SOURCE PREPARATION

A. ^{203}Tl(p,3n)^{201}Pb

Most of the ^{201}Pb sources used in this study were produced by bombarding natural Tl foils (70% ^{205}Tl, 29.5% ^{203}Tl) with 27-MeV protons from the Michigan State University sector-focused cyclotron to induce the reaction, ^{203}Tl(p,3n)^{201}Pb. A typical bombardment time was ≈1 hr.

The principal contaminants in these sources were 52-h ^{203}Pb, 3.6-h ^{202m}Pb, and 67-min ^{204m}Pb. ^{204m}Pb was essentially eliminated and ^{202m}Pb considerably reduced in these sources by aging them for 12 to 18 h prior to counting. 52-h ^{203}Pb was by far the most significant contaminant in these sources. Actually, ^{203}Pb usually accounted for more of the source activity than ^{201}Pb and its strength was enhanced with respect to 9.4-h ^{201}Pb by aging the sources. Fortunately, the decay of ^{203}Pb has been well studied and only three γ rays are emitted in its decay,[13] which were confirmed again in the present study. The biggest problem caused by this contaminant was to increase the Compton background for energies below 279 keV, thereby making it more difficult to observe weak γ rays in this region. Toward the end of our experiments we did make one source using enriched ^{203}Tl (70% ^{203}Tl, obtained from Oak Ridge National Laboratory), and the ^{203}Pb activity in this source was substantially reduced.

Simply aging the sources, however, did not completely eliminate the problem of source purity, for the Tl daughters of ^{201}Pb and ^{202m}Pb, 73-h ^{201}Tl and 12-d ^{202}Tl, are also γ-ray emitters. Therefore, we always performed a chemical separation of the Pb activity from the Tl target at the end of the aging period prior to counting. The Tl target was dissolved in the smallest possible amount of 6*N* HNO_3; 5 mg Pb^{++} carrier and 5 mg Hg^{+++} hold-back carrier were then added, followed by a small amount of 6*M* H_2SO_4 which precipitated the Pb activity as $PbSO_4$. After washing the precipitate with 2*M* H_2SO_4, it was dissolved in hot conc. H_2SO_4. The conc. H_2SO_4 solution was then diluted with two volumes of H_2O to which 5 mg of both Hg^{++} and Tl^{+++} hold-back carriers had been added. This again precipitated $PbSO_4$. The precipitate was again washed several times with 2*M* H_2SO_4 to which small amounts of Hg^{++} and Tl^{+++} carriers had been added. The $PbSO_4$ precipitate was then placed in a thin-wall glass vial for counting.

In order to keep the ratio of ^{201}Pb to ^{203}Pb as high as possible, sources made from a given Tl target were counted for only 5-12 h before being replaced by sources from another target (except for the experiments that followed the half-lives of the γ rays, in which the sources were counted longer).

B. ^{203}Tl(^{3}He,5*n*)^{201}Bi & ^{201}Pb

In an attempt to obtain ^{201}Pb sources containing less of the ^{203}Pb contaminant, several sources were prepared using an ion-exchange milking procedure, which took advantage of the difference in half-lives between 1.8-h ^{201}Bi and 11.8-h ^{203}Bi. Natural Tl was bombarded with a 48-MeV ^{3}He beam to induce the ^{203}Tl(^{3}He,5*n*)^{201}Bi reaction. The Tl target was dissolved in the minimum possible amount of 6*N* HNO_3 and then evaporated to dryness. The residue was dissolved in a small amount of conc. HCl, and this solution was evaporated to dryness after which the residue was again dissolved in conc. HCl (≈10 ml). Tl was removed from the solution by several extractions with diethyl ether saturated with conc. HCl. The aqueous phase containing Bi activity was then concentrated to about 1 ml and placed on a Dowex-1 anion-exchange column. The column was washed several times with 0.1*N* HCl, leaving a very clean source of Bi activity. The Pb activity, resulting from ε decay of the Bi, was allowed to build up in the ion-exchange column for ≈4 h before it was washed off with 0.1*N* HCl. This Pb activity was then aged ≈12 h, after which the remaining Pb was separated from the Tl daughters by the precipitation procedure described in §II.A. The source was then ready for counting.

III. EXPERIMENTAL RESULTS

A. γ-Ray Singles Spectra

^{201}Pb γ-ray singles spectra were obtained using two five-sided trapezoidal Ge(Li) detectors (0.42% and 2.5% efficient, relative to a 7.6×7.6-cm NaI(Tl) detector at 1332 keV and a source-to-detector distance of 25 cm) and a true coaxial Ge(Li) detector (3.6% efficient), having resolutions at 1332 keV of 3.0, 2.3, and 2.1 keV, respectively. The data were recorded by 4096-channel analyzers and by 4096- and 8192-channel ADC's coupled to PDP-9 and XDS Sigma-7 computers, respectively. For more details on data collection and reduction, see Refs. 14 and 15.

Figure 1 shows a γ-ray singles spectrum obtained with the 3.6% Ge(Li) detector in a 24-h period using a source prepared by the $(p,3n)$ reaction on enriched ^{203}Tl. The energies and intensities of the transitions were determined by means of a spectrum-analysis routine employing a live-display computer program. The γ-ray energies were measured by counting the ^{201}Pb sources simultaneously with various combinations of the energy standards listed in Table I.

In addition to the normal singles experiments, we performed an anti-Compton singles experiment using a 20.3×20.3-cm NaI(Tl) annulus in conjunction with the 2.5% efficient Ge(Li) detector. The anti-Compton experimental setup has been described previously

by Auble et al.[16] Because of the substantial reduction in Compton background effected in these spectra, we were able to obtain improved relative intensities for the weak low-energy γ rays.

After analyzing numerous singles spectra taken with different detectors and under varying conditions, we have been able to assign a total of 73 γ transitions (plus the 58.92-keV transition; cf. §E below) to the decay of ^{201}Pb. The energies and intensities of these γ rays are listed in Table II.

In 1971 Hnatowicz, Kristak, and Connor[17] reported energies and intensities for 55 γ transitions in the decay of ^{201}Pb. While their results are generally in agreement with ours, they report several transitions which we did not observe or which we have assigned to background or source impurities. These γ rays are listed in Table III along with our limits on the intensities.

Of the 32 γ transitions assigned to ^{201}Pb decay by Aasa et al.[12] from their conversion-electron measurements, we have confirmed 26. Our upper limits on the photon intensities of the six unobserved transitions are also given in Table III. These six transitions will be discussed further in §III.E., where it will be shown that the 225.4-, 760.7-, 815.3-, and 820.3-keV transitions have probably been incorrectly assigned to ^{201}Pb decay.

B. Anticoincidence and Integral Coincidence Spectra

Figure 2 shows the spectrum obtained using the 2.5% Ge(Li) detector in an anticoincidence arrangement with the 20.3×20.3-cm NaI(Tl) annulus and a 7.6×7.6-cm NaI(Tl) detector.[16] The single-channel analyzers associated with the NaI(Tl) detectors were set to

accept only γ rays above 100 keV in order to eliminate the Tl x-rays. The coincidence resolving time (2τ) was set at ≈100 nsec. The resulting γ-ray intensities are included in Table II, where they can be compared with the results of the singles and integral coincidence experiments. To facilitate the comparison of these intensities, the 1277-keV transition has been assigned a relative intensity of 100 in all three cases. The intensities listed for the integral coincidence experiment were obtained from the spectrum shown in Fig. 3. This spectrum was recorded by the 2.5% detector in the two-dimensional γ-γ coincidence experiment described in the next section.

In an anticoincidence spectrum there is a reduction in the intensity of cascade transitions, or, alternatively, ground-state transitions fed directly by ε decay are enhanced; whereas, in an integral coincidence spectrum, cascade transitions are enhanced with respect to ε-fed ground-state transitions. These spectra, therefore, can be used to identify certain γ rays which decay directly to the ground state, immediately implying the existence of certain energy levels. In the present case, we were able to propose states in ^{201}Tl at 1098.4, 1157.4, 1238.8, 1277.1, 1401.2, 1445.8, 1479.9, 1617.4, 1639.5, 1672.0, and 1755.3 keV solely on the basis of these two coincidence experiments.

C. Two-dimensional γ-γ Coincidence Spectra

To aid in the placement of the remaining γ rays in a consistent level scheme, we employed a two-parameter γ-γ ("megachannel") coincidence spectrometer system of 4096×4096 channels.[14] Using the 3.6% detector in coincidence with the 2.5% detector we accumulated ≈4 million pairs of coincidence events on magnetic tape in a 48-h period. A few examples of the ≈200 gated coincidence spectra used in the construction of the level scheme are shown in Fig. 4. A more complete selection of these gated spectra can be found in Ref. 18. A summary of the coincidence relationships deduced from these spectra is given in Table IV.

D. The 946-keV Doublet

A 946-keV transition was first reported in the decay of ^{201}Pb by Bergkvist et al.,[8] who measured its conversion electrons with a magnetic β spectrometer having 0.3% momentum resolution. Based on e^--γ coincidence experiments which showed that the 945.8-keV γ transition was in coincidence with the 331-keV γ but not with the 361-keV γ, Pettersson et al.[11] placed this rather strong transition between the 331.15- and 1277.1-keV levels. However, in our two-parameter γ-γ coincidence experiment we noticed that in addition to the large 331-keV coincidence peak, there was also a weak 361-keV peak in the 946-keV gated coincidence spectrum. We also observed peaks at about 946 keV in the 361- and 692-keV gated spectra. Based on these coincidence results, we concluded that the 946-keV

peak was probably a doublet, with the more intense γ ray feeding the 331-keV state and the weaker γ ray feeding the 692-keV state. The doublet nature of this transition was further demonstrated in the following two experiments.

The first experiment consisted of gating on the low, middle, and high energy parts of the 946-keV peak. In order to obtain approximately equal statistics for these three spectra, the number of channels used for these gates was chosen so that each spectrum would contain the same number of counts after subtracting the background. Therefore, the lower- and higher-energy gates contained more channels than the middle-energy gate, but all contained approximately the same number of coincidence events. From the resulting spectra, it appeared that the 361-keV peak became more pronounced as the gate moved from the low- to the high-energy side of the 946-keV peak. This indicated that the 946-keV peak was indeed a doublet, with the γ ray feeding the 692-keV level being somewhat higher in energy than the more intense γ ray feeding with the 331-keV level.

In the second experiment we obtained the energies of these two transitions using the "centroid shift" method. According to our decay scheme, the 124-, 203-, and 395-keV γ's, all of which feed the 1277.1-keV level, should be in coincidence with only the more intense, lower-energy component of the doublet, while the 361- and 692-keV γ's should be in coincidence with only the weaker, higher-energy component of the doublet. The gated spectra in coincidence with each component of the doublet were separately summed and the

two resulting spectra, as well as the integral coincidence spectra, were analyzed using the full peak width to determine the centroids. The shift in the centroid of the 946-keV peak was found to be 1.3±0.5 channels, which corresponds to an energy difference of 0.82±0.32 keV. As can be seen in Fig. 5, the centroids of the integral coincidence peak and the lower energy component of the doublet are very close, falling well within the calculated uncertainties of the centroids. Because of this and the fact that the lower-energy component is very much stronger, we assumed that the energy determined for the 946-keV doublet in the energy calibration experiment, 945.96 keV, was essentially that of the stronger peak. Based on this assumption, the energy of the higher energy peak was calculated to be 946.78±0.32 keV.

We were also able to obtain rough relative intensities for the two γ transitions from the areas of the 331- and 361-keV peaks appearing in the full 946-keV gated spectrum. We found that ≈6.2% of the composite 946-keV transitions feeds the 692-keV level, while 93.8% directly feeds the 331-keV state. The intensities listed in Table II were then obtained by multiplying the total γ-transition intensity of the 946-keV doublet by these percentages.

E. Conversion Coefficients

Prior to the present study, only three conversion coefficients had been measured for γ transitions in the decay of ^{201}Pb. These were the *K*-conversion coefficients for the 331- (α_K=0.113±0.008),

361- (α_K=0.21±0.025), and 585-keV (α_K=0.06±0.01) transitions, obtained by Pettersson et al.[11] from e^--γ coincidence data. However, relative K-conversion intensities had been measured for many γ transitions by Aasa et al.[12], so by combining these with our photon intensities, we were able to obtain K-conversion coefficients for 25 transitions. The two sets of relative intensities were normalized using the K-conversion coefficient of the 331-keV transition measured by Pettersson et al. The resulting conversion coefficients are given in Table V along with the calculated values of Hager and Seltzer[19] and our proposed multipolarities. Note that the α_K's determined here for the 361- and 585-keV transitions, 0.22±0.02 and 0.051±0.006, respectively, are in excellent agreement with those measured by Pettersson et al. Figure 6 shows graphically the theoretical α_K's together with the experimental points. The uncertainties associated with these points are based on the uncertainties in both photon and electron intensities, as well as the uncertainty in the fiducial point.

The experimental conversion coefficients are in good agreement with the theoretical conversion coefficients for $M1$, $E2$, and mixed $M1$+$E2$ multipolarities for all transitions listed in Table V, with the exception of the 308.9- and 753.4-keV transitions. Based on the measured K-conversion coefficients, the 308.9-keV transition could be mixed $E1$+$M2$ or $E0$+$E2$(+$M1$), while the 753.4-keV transition could be $M2$ or $E0$+$E2$(+$M1$). As we shall discover later, the $M2$ possibility for the 753.4-keV transition can be definitely ruled

out because of its placement in the decay scheme, and while an $E1$+$M2$ multipolarity cannot be definitely excluded for the 308.9-keV transition based on the decay scheme, it is very unlikely. However, as we did not attempt to confirm the conversion-electron intensity measurements, we are reluctant to assign the $E0$ component to either of these transitions at this time.

We can also make some speculations about the multipolarities of the six transitions observed by Aasa et al. for which we have only upper limits on the photon intensities (cf. Table III). Using these electron and photon intensities, we obtain the following lower limits on the conversion coefficients of these transitions: γ_{59} ($e_L/\gamma \geq 1.9$), γ_{167} ($e_K/\gamma > 0.5$), γ_{225} ($e_K/\gamma > 1.0$), γ_{761} ($e_K/\gamma > 1.2$), γ_{815} ($e_K/\gamma > 0.5$), and γ_{820} ($e_K/\gamma > 1.0$). Based on these conversion coefficients and the theoretical conversion coefficients of Hager and Seltzer, we come to the following conclusions regarding the possible multipolarities of these transitions: (1) If there is a 58.92- or 166.7-keV transition, it cannot have a multipolarity of $E1$ or $E2$; however, it may be $E0$, $M1$, or higher multipolarity. (2) The 225.4-keV transition would have to be $E0$, $M2$, or higher multipolarity. (3) The 760.7-, 815.3-, and 820.3-keV γ's would have to be $E0$ transitions. Although we cannot rule out the possibility of $E0$ or higher-multipole transitions, it seems more likely that the 225.4-, 760.7-, 815.3-, and 820.3-keV γ's have been incorrectly assigned to ^{201}Pb by Aasa et al. Although the existence of a 166.7-keV transition remains an open

question, the fact that the 58.92-keV transition can be placed in our decay scheme between two well established levels lends support to the assignment of this transition to ^{201}Pb.

IV. DECAY SCHEME

A. Level Placements

The level scheme for ^{201}Tl deduced from our coincidence studies, energy sums, and transition intensities is shown in Fig. 7. In this section we will present a brief summary of the evidence supporting these levels.

Previously established levels. The level scheme of Aasa et al.[12] proposed levels at 331, 692, 753, 932, 1098, 1157, 1239, 1277, 1401, and 1480 keV. Our results confirmed all of these levels except for those at 753 and 932 keV. The 753-keV level was based on the supposition that the 753-keV transition went directly to the ground state; however, our gated coincidence spectra show that the 753-keV transition is in strong coincidence with transitions deexciting the 962-keV level. The 932-keV level was proposed on the basis of population by 167-, 225-, and 345-keV transitions from levels at 1098, 1157, and 1277 keV, respectively, and its depopulation by an unobserved 239-keV transition. Since we have not observed the 167-, 225-, or 239-keV γ rays in our study and the 345-keV transition has been placed elsewhere in the decay scheme, we conclude that this proposed level at 932 keV does not exist.

1445.8-, 1639.5-, 1672.0-, and 1755.3-keV levels. The first piece of evidence for these levels came from the integral and anticoincidence experiments in which we identified ϵ-fed ground state

transitions from these levels. The placement of these levels was confirmed by the gated coincidence results which show transitions from all of these levels to the 331- and 692-keV levels.

1134.8-, 1290.0-, 1420.0-, and 1575.1-keV levels. Placement of the 1134.8-keV level was based on the results of the 803-keV gated coincidence spectrum. The relative intensities of the peaks in this spectrum indicated that the 803-keV γ populated the 331-keV level directly, and the resulting level at 1135 keV was populated directly or indirectly by the 130-, 155-, 285-, and 345-keV γ's. Additional evidence for this level came from the 345-keV gated coincidence spectrum which contained only two peaks, of equal intensity, at 331 and 803 keV. This agreed with the placement of the 345-keV γ between the previously established level at 1480 and the new level at 1134.8 keV.

The primary evidence for the level at 1290.0 keV came from the 598-keV gated coincidence spectrum, which indicated that the 598-keV transition directly populates the 692-keV level. Other gated coincidence spectra supported the placement of the 155.3-keV transition between the 1290.0- and 1134.8-keV levels, thereby increasing our confidence in both levels.

The facts that the strong 1089-keV transition was found to be in coincidence with only the 331-keV γ and that the 727-keV gated coincidence spectrum contained only the 331- and 361-keV γ's provided convincing evidence for the placing of the 1420.0-keV level.

The 285.0-keV transition was first placed between the 1420.0- and 1134.8-keV levels on the basis of energy sums. Although this

was consistent with the observation of 331- and 804-keV peaks in the 285-keV gated coincidence spectrum, it was not consistent with the observation of additional peaks at 155, 361, 598, and 692 keV. This discrepancy was resolved by proposing a new level at 1575.1 keV depopulated by a 285-keV γ. However, the intensities of the 285-keV peaks in the 598- and 804-keV gated spectra were inconsistent with the placement of the total intensity of the 285-keV γ between the 1575.1- and 1290.0-keV levels. We have therefore concluded that the 285-keV peak reported in Table II is a doublet with approximately half the intensity belonging to the transition between the 1420.0- and 1134.8-keV levels and the remaining intensity associated with the transition between the 1575.1- and 1290.0-keV levels.

Independent verification of three of the above levels, those at 1290.0, 1420.0, and 1575.1 keV, came from the $^{203}Tl(p,t)$ reaction work of Cleary, King, Maurenzig, and Stein.[20]

1330.4- and 1617.4-keV levels. The 1330.4-keV level was based primarily on the results of the 999-, 638-, and 232-keV gated coincidence spectra which showed that γ rays of these energies directly populate the 331.15-, 692.40-, and 1098.4-keV levels, respectively. The 1330.5-keV ground-state transition was placed on the basis of its energy, which agrees very well with the energy sums for the other transitions depopulating this level.

The 1617.4-keV level placement is supported by a ground-state transition that was shown to be c fed in the anticoincidence experiment. In addition, the 1286.3-keV transition was placed

between the 1617.4- and 331.15-keV levels on the basis of its energy and the observation of a very weak 331-keV peak in the 1286-keV gated spectrum.

1550.5- and 1712.5-keV levels. The evidence for these levels is limited and we have indicated our lack of confidence in them by using dashed lines for the levels and transitions in Fig. 7.

The 1550.5-keV level was based on the observation of a weak 331-keV peak in the 1219-keV gated coincidence spectrum and a 1550.5-keV peak in the γ-ray singles experiment.

The level at 1712.5 keV was based on the observation of a weak 331-keV peak in the 1381-keV gated spectrum and the energy sums, 1019.8 + 692.4 = 1712.2 keV and 1381.4 + 331.1 = 1712.5 keV. Unfortunately, the 1019.8-keV transition was so weak that we could not observe it in any of the coincidence spectra.

This concludes our discussion of the level placements except for a few words regarding the completeness of this level scheme. We have been able to place 65 of the 73 γ rays observed in our singles experiments (plus the 58.92-keV transition) in this decay scheme, and these account for more than 99.95% of the total γ-ray intensity. The eight γ rays left unplaced are all very weak, and their assignment to ^{201}Pb is not definite in most cases.

B. log*ft* Values

The total transition intensities were calculated from our γ-ray singles intensities and the theoretical conversion coefficients of Hager and Seltzer.[19] We assumed an *M*1 multipolarity for all transitions except those shown to be *E*2 or mixed *M*1+*E*2 by the measured conversion coefficients listed in Table V and those that would be *E*2 according to the final spin assignments. The total transition intensities, in percent of the total ^{201}Pb disintegrations, are given in the decay scheme, Fig. 7. The total intensity for the 58.92-keV transition was obtained using the *L* conversion-electron intensity given in Table III and theoretical conversion coefficients for an *M*1 transition.

From the measured *K* x-ray intensity listed in Table II, fluorescence yield (ω_K=0.97),[21] relative feedings to the excited levels and theoretical electron-capture shell ratios,[22] the total feeding to the ground state was calculated for two values of the decay energy. Using the decay energy of 1.8 MeV estimated by Wapstra and Gove,[23] we find a negative feeding to the ground state; however, if we take the maximum uncertainty in the measured x-ray intensity into account, we calculate an upper limit of 1.4%. Using the decay energy of 2.0 MeV obtained from the "experimental" masses of Myers and Swiatecki[24] we obtain a negative feeding even when using the maximum value for the x-ray intensity. Based on such calculations, we conclude that the ground-state feeding is probably in the range 0-1.4%.

The total ε feeding intensities to the excited states were calculated assuming no ground-state feeding, and these intensities are shown on the decay scheme to the right of the level energies. Logft values based on these ε-feeding intensities and a decay energy of 1.9 MeV are given to the right of the feeding intensities. The logft's were also calculated for decay energies of 1.8 and 2.0 MeV, and these are given in Table VI. This table demonstrates the extreme sensitivity of the logft's for the higher levels to the choice of decay energy.

C. β^+ Decay

In our singles spectra we observed a peak at 510.7 keV which appeared to be slightly broader than nearby γ-ray peaks. Considering the energy of this peak and its possible broadening, we have assumed it results from annihilation radiation from a β^+ decay branch of ^{201}Pb. From the relative intensities of the $\gamma^{\pm}$ radiation and the 331-keV transition listed in Table II, along with the total intensity for the 331-keV transition given in the decay scheme, we have calculated the total β^+ intensity from ^{201}Pb to be 0.05±0.01%.

If we assume the decay energy of either Wapstra and Gove[23] (1.8 MeV) or Meyers and Swiatecki[24] (2.0 MeV), the only states which can be populated by β^+ decay are the ground state and excited states at 331.15 and 692.40 keV. In Table VII we have summarized the theoretical β^+ feeding intensities for these levels using our ε-feeding intensities and theoretical ratios of ε/β^+.[22] This table shows that β^+ decay of ^{201}Pb should populate only the 331-keV

level to any significant extent and the decay energy is probably midway between 1.8 and 2.0 MeV if the theoretical ε/β^+ ratios are reasonably accurate. In fact, a calculation of the predicted β^+ feeding to the 331-keV level for a decay energy of 1.9 MeV yields a value of 0.053%, in excellent agreement with our measured value of 0.05±0.01%.

The fact that the β^+ decay primarily populates the 331.15-keV level is supported by the results of our γ-γ coincidence experiment. From Table IV we see that the 511-keV gated spectrum contained only a single peak at 331 keV. In addition, the 331-keV gated spectrum contained a strong peak at 511 keV which is absent in the 361- and 692-keV gated spectra.

The only previous report of positrons in the decay of ^{201}Pb indicated[25] two branches approximately 350 keV apart. Nothing was said concerning their relative intensities or which states they populate. Our experiments show that the major β^+ feeding goes to the 331.15-keV level and whether the other, much weaker branch observed by Bergkvist[25] goes to the ground state or the 692.4-keV level is still an open question. A complication also arises concerning the use of calculated ε/β^+ ratios, especially for transitions having large log ft values. It has been found[26] that even allowed (but retarded) transitions can have anomalous ε/β^+ ratios, and this can apparently be explained[27] by large second-order interference effects. Thus, any β^+ feeding to either the ground or 692.4-keV states might be difficult to predict accurately.

D. Spin and Parity Assignments

Ground state. The ground-state spin of ^{201}Tl has been measured in both atomic spectra[28] and atomic beam resonance[29,30] experiments to be 1/2. This is consistent with the predicted $s_{1/2}$ proton shell-model assignment for a single hole in the Z=82 closed shell, from which we obtain the positive parity assignment.

Although the ground-state spin of ^{201}Pb has not been measured directly, it was assumed to be $5/2^-$ as predicted by the shell model ($f_{5/2}$ neutron). Our upper limit of 1.4% on direct ε population of the ground state of ^{201}Tl is entirely consistent with a $5/2^-$ assignment for ^{201}Pb, as the calculated logf_1t of ≥9.5 is well above the minimum of 8.5 suggested by Raman and Gove[31] for first-forbidden unique transitions.

331.15-, 692.40-, and 1238.8-keV states. The $3/2^+$ assignments for the 331.15- and 1238.8-keV states are based on mixed *M*1+*E*2 transitions to the $1/2^+$ ground state. The $J^\pi=5/2^+$ for the 692.40-keV state is based on the assigned *M*1 multipolarity of the 361.25-keV transition and the angular correlation results of Pettersson et al.[11] This spin and parity is also consistent with the apparently "pure" *E*2 nature of the 692.40-keV transition as indicated by the experimental *K*-conversion coefficient.

The log*ft*'s for these three states as given in Table VI are all consistent with the assigned J^π's, since they are all first-forbidden nonunique transitions and require log*ft*'s ≥5.1.[31]

1098.4-keV state. The *M*1 multipolarities of the 406.0- and 767.3-keV transitions require $J^\pi=3/2^+$ or $5/2^+$, both of which are consistent with the log*ft* of 7.4. The multipolarity of the 1098.5-keV ground-state transition as derived from the measured *K*-conversion coefficient is *E*2+18(±17)%*M*1. If there is in fact an *M*1 component in the 1098.5-keV transition, the J^π of this state would be definitely $3/2^+$. Considering the large uncertainty in the *M*1 component, however, it is possible that the transition contains no *M*1 component, in which case the spin could be $5/2^+$. Based on the experimental results alone we are unable to make a definite assignment, although we do favor the $3/2^+$ assignment.

1134.8- and 1290.0-keV states. The *E*2 multipolarity of the 803.7-keV transition which goes to the 331.15-keV state ($J^\pi=3/2^+$) allows a choice of $1/2^+$, $3/2^+$, $5/2^+$, or $7/2^+$ for the 1134.8-keV state. The $1/2^+$ possibility was tentatively ruled out on the basis of the logf_1t, which lies in the range 8.0 (Q_ε=1.8 MeV) to 8.5 (Q_ε=2.0 MeV) and is somewhat low for a first-forbidden unique transition. Of the remaining possibilities, a spin of $7/2^+$ would give the simplest, although by no means the only, explanation of the apparently "pure" *E*2 nature of the 803.7-keV transition and the absence of a direct transition to the ground state. (The internal structures of the states must be known before such arguments can be very meaningful.)

In a recent study of ^{201}Tl using the ^{202}Hg(*d*,3nγ) reaction, Slocombe, Newton, and Dracoulis[32] obtained positive *A*2 and negative *A*4 angular distribution coefficients for the 803.7-keV transition, implying a stretched quadrupole transition. With this additional

evidence we are now fairly confident in assigning a J^π of $7/2^+$ to the 1134.8-keV state.

The $E2$ multipolarity of the 597.6-keV transition, which is placed between the 1290.0- and 692.40-keV levels, suggests a J^π of $1/2^+$, $3/2^+$, $5/2^+$, $7/2^+$, or $9/2^+$ for the 1290.0-keV state. The logft and logf_1t are consistent with any of these spins; however, the absence of γ transitions to the ground or 331.15-keV states suggests *tentatively* dropping the $1/2^+$, $3/2^+$, and $5/2^+$ possibilities. The remaining choices of $7/2^+$ and $9/2^+$ are supported by the ^{203}Tl(p,t) reaction work of Cleary et al.,[20] who observed a level at 1290±20 keV to which they tentatively assigned an l-transfer value of 4. Of these two possible spins, we prefer $9/2^+$ on the basis of the apparently "pure" $E2$ nature of the 597.6-keV transition and the large value of the logf_1t. Although the experimental evidence for our preferred assignment is tenuous, it is supported by the calculations of Covello and Sartoris[1] and Alaga and Ialongo[2] which will be discussed later.

1157.4-, 1277.1-, 1401.2-, 1445.8-, 1479.9-, 1639.5-, and 1672.0-keV states. The logft's for these seven states fall within the range for both allowed and first-forbidden nonunique ε transitions and thus limit the spins to 3/2, 5/2, or 7/2. The positive parities for all of these states were determined by at least one transition whose multipolarity was known and which populated a state whose parity had been identified previously. After eliminating $J^\pi=7/2^+$ because of the

transitions to the $1/2^+$ ground state, we are left with only the $3/2^+$ and $5/2^+$ possibilities for these seven states. Some of these can be narrowed as follows:

According to the angular correlation results of Pettersson et al.,[11] the spin of the 1277.1-keV state must be 1/2 or 3/2. Since we have already eliminated the spin of 1/2, it appears that the 1277.1-keV state is definitely $3/2^+$. However, because the angular correlation experiment was done with NaI(Tl) detectors and thus included some previously unresolved or unknown transitions in the energy gates, there is some question as to the validity of the results. Because of this we cannot eliminate the $5/2^+$ possibility, although we have indicated a definite preference for $3/2^+$ in our final decay scheme.

If the multipolarity of the 753.4-keV transition, which populates the 692.40-keV $5/2^+$ level, has an $E0$ component, as suggested by the experimental K-conversion coefficient, we could definitely assign the 1445.8-keV level a spin and parity of $5/2^+$. Unfortunately, as we have already mentioned in §III.E., we are very reluctant to assign an $E0$ component to this transition without additional evidence. We are therefore left with both the $3/2^+$ and $5/2^+$ possibilities for this state.

The 1479.9-keV level can be assigned a definite J^π of $5/2^+$ on the basis of the 345.0-keV $M1$ transition to the 1134.8-keV state ($J^\pi=7/2^+$).

The spins of the remaining states at 1157.4-, 1401.2-, 1639.5-, and 1672.0-keV have been narrowed to a choice between $3/2^+$ and $5/2^+$.

Based on the γ branching ratios from these four levels, we tend to favor slightly the $5/2^+$ possibilities, which is why $5/2^+$ is placed before $3/2^+$ on these levels in Fig. 7. However, it should be emphasized that γ branching ratios can be misleading if the internal structures of the states are not known, so these are only weak preferences.

1330.4-, 1550.5-, 1617.4-, and 1755.3-keV states. The log*ft*'s for these states allow spin assignments of 3/2, 5/2, and 7/2. We can very confidently eliminate the 7/2 spin on the basis of the γ transitions to the $1/2^+$ ground state. A $5/2^-$ assignment is also unlikely, as this would mean *M*2 transitions to the ground state competing significantly with *E*1 transitions to the $3/2^+$ and $5/2^+$ states. Our final choice for all four states is thus narrowed to $3/2^\pm$ or $5/2^+$.

1420.0-, 1575.1-, and 1712.5-keV states. Spin assignments of 3/2, 5/2, or 7/2 are again suggested by the log*ft*'s for these three states.

The parity of the 1420.0-keV state can be tentatively identified as positive from the probable *M*1 nature of the 285.0-keV γ transition to the positive parity state at 1134.8 keV. The absence of a transition to the $1/2^+$ ground state, coupled with the transitions to the $7/2^+$ and $9/2^+,(7/2^+)$ states implies a probable J^π of either $5/2^+$ or $7/2^+$ for the 1420.0-keV state. (A J^π of $5/2^-$ is also possible considering the uncertainty of both the spin of the 1290.0-keV state and the multipolarity of the 285.0-keV transition.)

The only γ transition observed from the 1575.1-keV state goes to the $9/2^+,(7/2^+)$ state at 1290.0 keV. The probable *M*1 multipolarity for this 285.0-keV transition allows us to make a tentative assignment of $7/2^+$ for this state, although $5/2^\pm$, $7/2^-$, and $3/2^+$ assignments are also quite possible considering the uncertainty of both the spin of the 1290 keV state and the multipolarity of the 285.0 keV γ transition.

The 1712.5-keV state is depopulated by only two γ transitions, which go to the $3/2^+$ and $5/2^+$ states at 331.15- and 692.40-keV, respectively. The transition to the $3/2^+$ state makes a $7/2^-$ assignment very unlikely for this state, since we would again have an *M*2 transition competing strongly with *E*1 transitions. Although the absence of a transition to the $1/2^+$ ground state may suggest a preference for the $7/2^+$ and $5/2^-$ assignments, this is a very weak argument and we are left with the following possibilities for the 1712.5-keV state: $3/2^\pm$, $5/2^\pm$, and $7/2^+$.

V. DISCUSSION AND INTERPRETATION OF ^{201}Tl STATES

A. Shell-Model Description

^{201}Tl lies only six neutrons short of the N=126 closed shell and one proton short of the Z=82 closed shell, so we expect it to be a spherical nucleus, at least at low energies, describable in terms of the simple shell model. (Cf., however, the work of Newton et al.,[33] in which some moderate-energy, high-spin states in ^{199}Tl are interpreted as members of a rotational band. Some states in nuclei in this region have also been interpreted as triaxial states.[34]) In the simplest model the neutrons are completely paired and the nuclear properties are determined solely by the odd proton (hole). For ^{207}Tl with its closed neutron shell this is a reasonable description, and its states, up to fairly high energy, can be identified with specific one-proton-hole states. These states up to 1.8 MeV are shown in Fig. 8, along with the known states of other neutron-deficient odd-mass Tl isotopes.[35] The $1/2^+$, $3/2^+$, $11/2^-$, $5/2^+$, and $7/2^+$ states consist primarily of $s_{1/2}$, $d_{3/2}$, $h_{11/2}$, $d_{5/2}$, and $g_{7/2}$ components, respectively, corresponding to the inverse order of proton filling between the Z=50 and 82 closed shells. (The $7/2^+$ state lies at 3.48 MeV and thus does not appear in Fig. 8.) The electromagnetic properties, β-transition rates, and single-neutron transfer spectroscopic factors all indicate that these are fairly pure single-particle states.[35]

As one progresses from ^{207}Tl to the lower-mass Tl isotopes, the N=126 shell loses more and more neutrons, so the "non-interacting" neutron description becomes more and more of an approximation. Many properties remain similar to ^{207}Tl, however: As can be seen in Fig. 8, the ground states of all the odd-mass isotopes remain $1/2^+$. Likewise, the first-excited states all lie very close in energy and remain $3/2^+$. One can thus reasonably assume that the ground and first-excited states of these isotopes, including ^{201}Tl, can be described as fairly pure $s_{1/2}$ and $d_{3/2}$ proton-hole states.

The second excited state in ^{207}Tl is the $h_{11/2}$ state at 1341 keV; although possible $11/2^-$ states have been observed in some odd-mass Tl isotopes close to this energy,[33,39] a number of additional states have been observed between the $d_{3/2}$ state and ≈1.3 MeV in all of these isotopes but ^{207}Tl. The second excited state in ^{205}Tl to ^{199}Tl has $J^\pi=5/2^+$. One might try to describe these states as $d_{5/2}$ shell-model states. However, the $d_{5/2}$ state (the third excited state) in ^{207}Tl lies at 1674 keV, and it would be difficult to explain the lowering of this state to ≈600-700 keV, where it appears in the lighter isotopes. In addition, proton pick-up reaction data[39] indicate relatively small single-proton amplitudes for these states in ^{205}Tl and ^{203}Tl, indicating a more complex structure for these than a single $d_{5/2}$ proton hole.

The third excited state in ^{201}Tl lies at 919.1 keV,[41] is not populated by the ε decay of ^{201}Pb, and has a probable J^π of $9/2^-$. It presents another serious problem for a single-particle description, as the lowest proton orbital giving rise to this J^π is the $h_{9/2}$

orbital, which lies above the Z=82 closed shell. A state arising from it would be expected to have an energy of ≈3.6 MeV. In addition to such difficulties, a single-particle model cannot account for the density of states observed just above 1 MeV, so we are forced to abandon this simple description in favor of a many-particle shell-model description.

Silverberg[44] has performed a shell-model calculation for ^{205}Tl in which he considered the nucleus as three proton holes moving in a static potential and interacting with one another by some residual force. While this approach qualitatively describes the low-lying ^{205}Tl states, the quantitative results were poor. And because they become more complex as one moves farther from the closed neutron shell, involving many-particle configurations and basis sets containing high-spin, high-multiplicity orbitals, no significant shell-model calculations have yet been performed for Tl nuclei lighter than ^{205}Tl. However, we can generalize some of Silverberg's results in a very qualitative way to the states in ^{201}Tl.

Applying the multi-particle shell model to ^{201}Tl, we can interpret the three lowest states as follows: The dominant configuration in the ground-state wave function should be $\{\pi(s_{1/2})^{-1}\ \nu[(p_{1/2})_0^{-2}(f_{5/2})_0^{-4}]_0\}_{1/2^+}$; in the 331.15-keV $3/2^+$ state, $\{\pi(d_{3/2})^{-1}\ \nu[(p_{1/2})_0^{-2}(f_{5/2})_0^{-4}]_0\}_{3/2^+}$. In analogy with Silverberg's ^{205}Tl results we postulate $\{\pi(s_{1/2})^{-1}\ \nu[(p_{1/2})^{-1}(f_{5/2})^{-5}_{5/2}]_2\}_{5/2^+}$ as a significant component in the 692.40-keV $5/2^+$ state, with only a small amplitude for $\{\pi(d_{5/2})^{-1}\ \nu[(p_{1/2})_0^{-2}(f_{5/2})_0^{-4}]_0\}_{5/2^+}$ -- although in this case we would expect an equally large admixture of other

configurations such as $\{\pi(s_{1/2})^{-1}\ \nu[(p_{1/2})_0^{-2}(f_{5/2})_2^{-4}]_2\}_{5/2^+}$, $\{\pi(s_{1/2})^{-1}\ \nu[(p_{1/2})_0^{-2}(p_{3/2})_2^{-2}(f_{5/2})_0^{-2}]_2\}_{5/2^+}$, and $\{\pi(s_{1/2})^{-1}\ \nu[(f_{5/2})_0^{-4}\{(p_{1/2})^{-1}(p_{3/2})^{-1}\}_2]_2\}_{5\ 2^+}$.

On a very qualitative level these configurations can be used to explain some properties of the low-lying states. The ε decay of ^{201}Pb to the ^{201}Tl ground state would involve the transition $\pi s_{1/2} \xrightarrow{\Delta l=3} \nu f_{5/2}$, which is consistent with our log$ft \geq 9.5$. The ε decay to the 331.15-keV state would be the simple transition $\pi d_{3/2} \xrightarrow{\Delta l=1} \nu f_{5/2}$ (logft = 6.7). And the fastest ε decay to the 692.40-keV state (logft = 7.4) would go by $\pi s_{1/2} \xrightarrow{\Delta l=1} \nu p_{1/2}$, which means the primary component of the 692.40-keV state's wave function involved is $\{\pi(s_{1/2})^{-1}\ \nu[(p_{1/2})^{-1}(f_{5/2})^{-5}_{5/2})_2\}_{5/2^+}$, since the other major components would involve complex or more hindered transitions such as $\pi s_{1/2} \rightarrow \nu f_{3/2}$. The different log$ft$ values for the transitions to the 331.15-keV state (6.7) and the 692.40-keV state (7.4) could then be explained by the fact that the former is fairly pure, whereas the latter is highly admixed with configurations that contribute relatively little to the ε strength.

The large *E*2 component of the 331.15-keV γ transition between the $3/2^+$ and $1/2^+$ states can also be explained by our proposed configurations, for they involve a simple $\pi d_{3/2} \xrightarrow{\Delta l=2} \pi s_{1/2}$ transition, an *l*-forbidden *M*1. The strong 361.25-keV γ transition between the $5/2^+$ and $3/2^+$ states cannot be explained by the above configurations because they would all involve a $\pi s_{1/2} \xrightarrow{\Delta l=2} \pi d_{3/2}$ transition and a simultaneous neutron transition. However, by introducing a small

component of $\{\pi(s_{1/2})^{-1}\ \nu[(p_{1/2})^{-1}(f_{5/2})^{-5}_{5/2}]_2\}_{3/2^+}$ into the 331.15-keV wave function, the γ transition can be nicely explained.

It is rather obvious from our discussion thus far that even among the low-lying states of ^{201}Tl configuration mixing is substantial and that more complex, complete shell-model calculations will be necessary before even a reasonably complete description of the states can be given. It will be instructive to consider the weak-coupling model as an alternative in the next section.

B. Weak-Coupling (Core-Coupling) Description

In addition to performing the three-particle shell-model calculations on ^{205}Tl mentioned above, Silverberg[44] calculated this same nucleus as a single proton hole coupled to a vibrating core and concluded that this later calculation provided a satisfactory description of this nucleus with considerably less numerical work. Since this work was published in 1961 several additional studies have been made of the odd-mass Tl isotopes using the intermediate-coupling unified model,[1-3] and two of these included calculations for ^{201}Tl.[1,2] These calculations are of particular interest to us as they give us a chance to compare our proposed level scheme with this numerically simple model.

Since a complete description of the unified model on which much of this description is based exists elsewhere,[45] we will restrict ourselves here to a comparison of the assumptions and parameters used in the calculations by Covello and Sartoris[1] and Alaga and Ialongo.[2] In their calculation, Covello and Sartoris[1] considered all the proton-

hole orbitals within the shell ending at $Z=82$, namely, $3s_{1/2}$, $2d_{3/2}$, $1h_{11/2}$, $2d_{5/2}$, and $1g_{7/2}$, and included all the core states up to three phonons. Alaga and Ialongo[2] however, used only the $3s_{1/2}$, $2d_{3/2}$, $1h_{11/2}$, and $2d_{5/2}$, shell-model states but also included vibrator states up to three phonons.

The two parameters which specify the collective motion of the core and its interaction with the motion of the hole are the phonon energy, $\hbar\omega$, and the strength of the surface-hole coupling, η or α. The phonon energy is deduced for each odd-mass Tl isotope from the neighboring even isotope (for ^{201}Pb this is taken to be the first 2^+ state in ^{202}Pb at 960 keV). The coupling constant is treated as a free parameter to be varied within reasonable limits. Although both calculations used the same value for $\hbar\omega$, 960 keV, the coupling constant which gave the best fit to the existing experimental data was different, as one might expect.

Another difference between these calculations has to do with the assumption made concerning the single-hole excitation energies, $\Delta_j = \varepsilon_j - \varepsilon_{1/2}$. Alaga and Ialongo assumed these energies were fixed and equal to the excited single-particle states in ^{207}Tl. However, Covello and Sartoris state that these energies cannot be taken from the experimental spectrum of ^{207}Tl because these experimental energies should be corrected for the interaction with the core, which is also effective in ^{207}Tl. Furthermore, the interaction between the odd hole and the core contains a short-range part, which has not been included in the model Hamiltonian. This short-range part of the force would act in first-order perturbation theory as a renormalization of the

single-hole energy spectrum, thus producing effective spacings peculiar to each isotope. Because of this they considered the quantities Δ_j as adjustable parameters for all levels except the $g_{7/2}$ level, which is so high in energy that any change in its position due to these corrections is irrelevant, and they took $\Delta_{7/2}$ from the ^{207}Tl $7/2^+$ level.

In Fig. 9 the energy levels calculated by Covello and Sartoris[1] (CS) are compared with those calculated by Alaga and Ialongo[2] (AI), and both of these are compared to the ^{201}Tl levels found experimentally in this work.

With the exception of the $9/2^-$ state at 919.1 keV, the known level structure below 1 MeV is reproduced fairly well in both calculations. However, because of the many states observed in our decay scheme between 1 and 2 MeV, it is difficult to draw a correspondence between the experimental and theoretical states in this region. This difficulty is compounded by the uncertainty in the spins of many of these states. Fortunately, these authors included calculations of the electric quadrupole and magnetic dipole reduced matrix elements for some states. From the $B(E2)$'s and $B(M1)$'s we were able to calculate γ-ray multipolarity mixing ratios, δ^2, as well as γ-branching ratios. The results are given in Tables VIII and IX, where they are compared with the experimental results which were found to give the best agreement.

The agreement between the calculated and measured energy of the $(3/2^+)_1$ level is quite good, and the large $E2$ admixture in the 331.15-keV transition is well reproduced in the calculations, especially that of AI.

The energy calculated by CS for the $(5/2^+)_1$ state, 722 keV, is in much better agreement with experiment than the 620 keV calculated by AI, while the experimental γ branching from this level is in better agreement with the latter calculation. Both calculations predict a very small $E2$ admixture in the 361.25-keV transition, which agrees with our experimental results.

Both calculations predict a $7/2^+$ state at $\simeq$1050 keV as the third excited state. Experimentally, the third excited state at 919.1 keV has J^π of $9/2^-$, while the calculations do not predict a $9/2^-$ state below at least 2.2 MeV. The lowest lying $7/2^+$ state found experimentally lies at 1134.8 keV. Based on the agreement between the calculated and experimental γ-branching ratios from this level, we are fairly confident that the calculated $(7/2^+)_1$ state corresponds to our state at 1134.8 keV.

The next state predicted by the calculations has a J^π of $3/2^+$ and lies at 1125 keV (CS) or 1193 keV (AI). There are four experimental levels within 100 keV of these energies which have possible J^π's of $3/2^+$. Of these, only the 1098.4-keV level has an experimental γ-branching pattern consistent with that of the calculated $(3/2^+)_2$ state. In addition, the $E2/M1$ mixing ratios for the 767.3- and 1098.5-keV γ rays which deexcite this level are in excellent agreement with those obtained from the calculations of AI. We thus conclude that the predicted $(3/2^+)_2$ state corresponds to our $3/2^+$ state at 1098.4 keV.

The next predicted state has a J^π of $5/2^+$ and lies at 1299 keV (CS) or 1344 keV (AI). Although there are 14 experimental states

found between 1157.4 and 1755.3 keV which may have a J^π of $5/2^+$, the predicted γ-branching pattern did not fit any of these well enough to draw a correspondence. This may result from configuration mixing between the $(5/2^+)_2$ calculated state and some of the other possible $5/2^+$ states which are not predicted by the calculations.

CS predict a $1/2^+$ state at 1386 keV as the next state, while AI predict a $9/2^+$ state at 1420 keV, lower than the $(1/2^+)_2$ state at ≈1540 keV. As Fig. 9 indicates, no excited $1/2^+$ states have yet been observed in ^{201}Tl (although they would very likely not be populated via the ε of ^{201}Pb). Based on the γ-branching ratio to the $(7/2^+)_1$ and $(5/2^+)_1$ states, it appears that the $(9/2^+)_1$ state predicted by AI corresponds to our state at 1290.0 keV. This reinforces our previous preferred J^π assignment of $9/2^+$ for this state.

Both calculations predict a $3/2^+$ state above the $(1/2^+)_2$ state, followed by yet another $5/2^+$ state. However, as no reduced transition probabilities were calculated for γ transitions from these states and since there are many possible $3/2^+$ and $5/2^+$ experimental states in the energy region predicted for these, we are unable to make a correspondence between the calculated states and any of our experimental states.

CS predict states up to the $(5/2^+)_3$ state, while AI continue to somewhat higher energies. They predict an $11/2^-$ state at 1780 keV and additional states above 2100 keV with J^π's of $11/2^+$, $7/2^+$, and $1/2^+$. None of these states can be associated with experiment at this time.

C. Rotational-Model Descriptions

As we have seen, the weak-coupling model gives a much better and simpler description of the ^{201}Tl level structure than the shell model, although neither description is able to account for the high density of states between 1 and 2 MeV. Both descriptions also fail to explain the low lying $9/2^-$ state at 919.1 keV. To explain this level Newton *et al.*[33] have suggested the possibility of an oblate deformation of the nucleus with the resultant lowering of the $9/2^-[505]$ Nilsson single-particle level from its position in the spherical case. This possibility has been supported in calculations by Uyttenhove *et al.*,[41] which show that for a slight oblate deformation a minimum occurs in the total potential energy for the $9/2^-[505]$ orbital. This raises the possibility of examining the level structure of ^{201}Tl in terms of various rotational models.

A number of low-lying high-spin negative parity states in ^{199}Tl have been described by Meyer-ter-Vehn[34] in terms of a triaxial-rotor-plus-particle model. In this model the $9/2^-$ state at 748.5 keV in ^{199}Tl has been described as an $h_{9/2}$ proton coupled to a triaxial core. This description could also be applied to the 919.1-keV state in ^{201}Tl.

High-spin negative-parity states in ^{201}Tl, including the $9/2^-$ state at 919.1 keV, observed in the ^{202}Hg$(d,3n\gamma)$ reaction by Slocombe, Newton, and Dracoulis,[32] have been interpreted in terms of a symmetric rotor-plus-particle model. These authors have also performed successful calculations for the low-lying positive-parity levels using this model.

The fact that relatively low-lying levels in ^{201}Tl may be amenable to interpretation in terms of rotational models suggests a nucleus much "softer" than one would have previously expected in this region so close to the double-closed shell of ^{208}Pb. Such states have also been found[45] in nuclides just below N=82, however, and entire rotational bands have been characterized[46] in nuclei within the $f_{7/2}$ shell. Thus, it appears that trying to characterize states in nuclei according to "simple" models is likely an oversimplification, even for nuclei quite near doubly closed shells.

Acknowledgements

We wish to thank members of the Nuclear Chemistry and Physics Groups at Michigan State University, both past and present, who helped in various ways with these experiments, especially Drs. R. A. Warner, G. C. Giesler, and K. L. Kosanke. Helpful discussions at Lawrence Berkeley Laboratory with Drs. E. Browne and L. J. Jardine are gratefully acknowledged. Finally, we wish to thank Dr. J. O. Newton for communicating results of the ^{202}Hg(d,3$n\gamma$) reaction study prior to publication. R.E.D. would like to acknowledge the support of the Lawrence Berkeley Laboratory during the final stages of manuscript production.

References

[1]A. Covello and G. Sartoris, Nucl. Phys. A93, 481 (1967).

[2]G. Alaga and G. Ialongo, Nucl. Phys. A97, 600 (1967).

[3]N. Azziz and A. Covello, Nucl. Phys. A123, 681 (1969).

[4]R. E. Doebler, Wm. C. McHarris, and W. H. Kelly, to be published.

[5]J. J. Howland, D. H. Templeton, and I. Perlman, University of California declassified report BC 31 (1946).

[6]H. M. Neumann and I. Perlman, Phys. Rev. 78, 191 (1950).

[7]A. H. Wapstra, D. Maeder, G. J. Nijgh, and L. Th. M. Ornstein, Physica 20, 169 (1954).

[8]K. E. Bergkvist, I. Bergström, C. J. Herrlander, S. Hultberg, H. Slätis, E. Sokolowski, A. H. Wapstra, and T. Wiedling, Phil. Mag. 46, 65 (1955).

[9]T. R. Gerholm, unpublished results quoted in Ref. 8.

[10]J. Lindskog, E. Bashandy, and T. R. Gerholm, Nucl. Phys. 16, 175 (1960).

[11]B. G. Pettersson, T. R. Gerholm, Z. Grabowski, and B. Van Nooijen, Nucl. Phys. 24, 196 (1961).

[12]E. Aasa, T. Sundström, O. Bergman, J. Lindskog, and K. Sevier, Ark. Fys. 27, 133 (1964).

[13]J. R. Prescott, Proc. Phys. Soc. (London) 67A, 254 (1954).

[14]R. E. Doebler, Wm. C. McHarris, and W. H. Kelly, Phys. Rev. C2, 2422 (1970).

[15]J. Guile, R. E. Doebler, Wm. C. McHarris, and W. H. Kelly, Phys. Rev. C5, 2107 (1972).

[16]R. L. Auble, D. B. Beery, G. Berzins, L. M. Beyer, R. C. Etherton, W. H. Kelly, and Wm. C. McHarris, Nucl. Instr. Methods 51, 61 (1967).

[17]V. Hnatowicz, J. Kristak, and R. D. Connor, Nucl. Phys. A175, 539 (1971).

[18]R. E. Doebler, Ph.D. Thesis, Michigan State University, 1970.

[19]R. S. Hager and E. C. Seltzer, Nucl. Data A4, 1 (1968).

[20]T. P. Cleary, C. H. King, P. R. Maurenzig, and N. Stein, private communication to Nuclear Data Group (December, 1970); Nucl. Data B5, 561 (1971).

[21]W. Bambynek, B. Crasemann, R. W. Fink, H. U. Freund, H. Mark, C. D. Swift, R. E. Price, and P. V. Rao, Rev. Mod. Phys. 44, 716 (1972).

[22]NUSPEC (Nuclear Spectroscopy Interactive Program Package), a computer program written by C. M. Lederer, A. Shihab-Eldin, and L. J. Jardine, described in IAEA document INDC(NDS)-61 W+spec. p. 156 (1974).

[23]A. H. Wapstra and N. B. Gove, Nucl. Data A9, 267 (1971).

[24]W. D. Myers and W. J. Swiatecki, University of California Lawrence Radiation Laboratory Report No. UCRL-11980 (1965).

[25]K. E. Bergkvist, private communication, quoted in I. Bergström and G. Andersson, Ark. Fys. 12, 415 (1957).

[26]R. B. Firestone, R. A. Warner, Wm. C. McHarris, and W. H. Kelly, Phys. Rev. Letters 35, 401 (1975).

[27]R. B. Firestone, Wm. C. McHarris, and B. R. Holstein, Phys. Rev. C, accepted for publication (1978).

[28]R. J. Hull and H. H. Stroke, Phys. Rev. 122, 1574 (1961); J. Opt. Soc. Am. 51, 1203 (1961).

[29]I. Lindgren, C. M. Johansson, and S. Axensten, Phys. Rev. Letters 1, 473 (1958).

[30]L. L. Marino, Bull. Am. Phys. Soc. 3, 186 (1958).

[31]S. Raman and N. B. Gove, Phys. Rev. C7, 1995 (1973).

[32]M. G. Slocombe, J. O. Newton, and G. D. Dracoulis, Nucl. Phys. A, to be published.

[33]J. O. Newton, N. Cirilov, F. S. Stephens, and R. M. Diamond, Nucl. Phys. A148, 593 (1970).

[34]J. Meyer-ter-Vehn, Nucl. Phys. A249, 111 (1975); A249, 141 (1975).

[35]P. D. Barnes, E. R. Flynn, G. J. Igo, and D. D. Armstrong, Phys. Rev. C 1, 228 (1970).

[36]J. Ungrin, R. M. Diamond, P. O. Tjom, and B. Elbeck, Kgl. Dan. Vidensk. Selsk., Mat.-Fys. Medd. 38, No. 8 (1971).

[37]R. Alberini, P. R. Oliva, D. Prosperi, Lett. Nuovo Cim. 10, 726 (1974).

[38]E. Barnard, W. Coetzee, J. A. M. deVillers, D. Reitmann, and P. Van der Merve, Nucl. Phys. A157, 130 (1970).

[39]S. Hinds, R. Middleton, J. H. Bjerregaard, O. Hansen, and O. Nathan, Nucl. Phys. 83, 17 (1966).

[40]C. Glashausser, D. L. Hendrie, and E. A. McClatchie, Nucl. Phys. A222, 65 (1974).

[41]J. Uyttenhove, K. Heyde, H. Vincx, and M. Waroquier, Nucl. Phys. A241, 135 (1975).

[42]R. M. Diamond and F. S. Stephens, Nucl. Phys. 45, 632 (1963).

[43]P. K. Hopke, H. Hubel, R. A. Naumann, E. H. Spejewski, and A. T. Strigachev, Nucl. Phys. A184, 497 (1972).

[44]L. Silverberg, Ark. Fys. 20, 355 (1961).

[45]R. B. Firestone, R. Aryaeinejad, and Wm. C. McHarris, to be published.

[46]L. E. Samuelson, W. H. Bentley, W. H. Kelly, R. A. Warner, F. M. Bernthal, and Wm. C. McHarris, Phys. Rev. C 15, 821 (1977).

Table I

γ Rays Used as Energy Standards

Nuclide	γ-Ray Energy (keV)	Reference
^{201}Tl	135.34 ±0.04	a
	167.43 ±0.07	a
^{203}Pb	279.191±0.008	b
^{198}Au	411.795±0.009	b
^{110m}Ag	446.77 ±0.04	c
	620.22 ±0.03	c
	657.71 ±0.03	c
	677.55 ±0.03	c
	686.80 ±0.03	c
	744.19 ±0.04	c
	763.88 ±0.04	c
	818.00 ±0.04	c
	884.67 ±0.04	c
	937.48 ±0.04	c
	1384.26 ±0.05	d
	1505.01 ±0.07	d
^{207}Bi	569.62 ±0.06	b
	1063.64 ±0.06	d

Table I

(Continued)

Nuclide	γ-Ray Energy (keV)	Reference
^{54}Mn	834.83 ±0.04	e
^{88}Y	898.03 ±0.04	e
	1836.13 ±0.04	e
^{182}Ta	1121.31 ±0.05	d
	1189.06 ±0.05	d
	1221.42 ±0.05	d
^{60}Co	1173.23 ±0.04	b
	1332.50 ±0.03	e

[a] C. J. Herrlander, R. Stockendal, and R. K. Gupta, Ark. Phys., 17, 315 (1960).

[b] J. B. Marion, Nuclear Data, A4, 301 (1968).

[c] S. M. Brahmavar, J. H. Hamilton, and A. V. Ramayya, Nucl. Phys., A125, 217 (1969).

[d] R. E. Doebler, Nuclear Chemistry Annual Report, Michigan State University, COO-1779-49 (1970).

[e] Average of b and f.

[f] R. Gunnink, R. A. Meyer, J. B. Niday, and R. P. Anderson, Nucl. Instr. Meth., 65, 26 (1968).

Table II

Energies and Relative Intensities of γ Rays from the Decay of ^{201}Pb

Measured Energies (keV)	Relative Intensities		
	Singles	Anticoincidence	Integral γ-γ Coincidence
K x-rays	4980 ±250	-	-
120.0 ±0.2	1.20± 0.30	-	30± 5
124.2 ±0.2	2.5 ± 0.5[a]	-	34± 5
129.95±0.10	6.4 ± 0.6[a]	-	114± 12
155.31±0.10	8.2 ± 1.0	6.0± 1.0	179± 15
202.79±0.10	4.0 ± 0.5	-	80± 10
231.87±0.10	6.5 ± 0.8	1.6± 0.5	106± 11
241.02±0.08	10.0 ± 1.0[a]	2.1± 0.5	139± 14
285.04±0.07[b]	10.3 ± 1.0	1.5± 1.0	166± 17
302.70±0.40[c]	0.65± 0.15	-	23± 5
308.93±0.15	2.3 ± 0.3	-	25± 5
322.42±0.15	4.4 ± 0.6	-	104± 15
331.15±0.06	4550 ±250	2800 ±150	20290±1000
341.51±0.08	6.8 ± 0.8	1.4± 0.6	85± 10
344.95±0.07	18.3 ± 1.5	5.0± 1.0	269± 20
361.25±0.06	560 ± 30	156 ±10	6730± 400
381.29±0.08	12.9 ± 0.7	3.5± 0.5	183± 15
394.86±0.09	10.8 ± 0.7	4.3± 1.0	213± 20
405.96±0.07	120 ± 6	33 ± 5	1717± 150
464.90±0.08	19.8 ± 1.0	5.4± 0.6	275± 20

Table II

(Continued)

Measured Energies (keV)	Relative Intensities		
	Singles	Anticoincidence	Integral γ-γ Coincidence
481.98±0.09	3.2 ± 0.6	-	53± 8
510.7 ±0.2($\gamma^{\pm}$)	6 ± 1	1.3± 0.3	31± 5
514.38±0.09	9.1 ± 2.0	1.6± 0.2	119± 15
540.90±0.09	16.2 ± 1.0	4.5± 0.7	238± 25
546.28±0.09	16.5 ± 1.0	4.4± 0.5	231± 25
562.81±0.10[c,d]	1.8 ± 0.4	-	-
584.60±0.08	211 ± 10	60.2± 3.0	2814± 200
597.60±0.09	19.0 ± 1.0	4.4± 0.2	303± 25
637.90±0.09	21.7 ± 1.0	6.3± 0.3	295± 25
692.41±0.08	254 ± 12	182 ±10	1365± 80
708.75±0.09	46.2 ± 2.0	14.5± 0.6	636± 50
727.50±0.09	7.1 ± 0.7	2.3± 0.2	93± 10
753.35±0.09	8.8 ± 0.8	2.6± 0.2	105± 15
767.26±0.08	194 ± 10	75.5± 4.0	1685± 150
787.29±0.10	34 ± 4[a]	13 ± 3	468± 100[a]
803.66±0.07	90 ± 6	23.3± 1.0	1184± 80[a]
826.26±0.08	141 ± 7	54.9± 3.0	1240± 80
907.67±0.08	362 ± 20	157 ± 8	2766± 140
945.96±0.08[e]	424 ± 30[e]	205 ±10	3460± 170
946.78±0.40[e]	28 ± 10[e]	-	-
979.4 ±0.3	1.1 ± 0.3	1,1± 0.4	21± 4

Table II
(Continued)

Measured Energies (keV)	Relative Intensities		
	Singles	Anticoincidence	Integral γ-γ Coincidence
999.23±0.07	38.3 ± 2.0	17.0± 1.0	327± 30
1010.3 ±0.3[c,d]	1.0 ± 0.2	-	6.8± 1.5
1019.8 ±0.3[c]	0.9 ± 0.4	-	16± 5
1062.79±0.15	4.0 ± 0.5	2.2± 0.2	57± 6
1070.04±0.08	71.8 ± 4.0	35.5± 2.0	516± 40
1088.85±0.09	53.2 ± 3.0	24.9± 1.5	378± 30
1098.52±0.07	111 ± 6	108 ± 6	173± 10
1114.73±0.08	9.8 ± 0.6	4.4± 1.0	82± 10
1124.9 ±0.2[c,d]	0.57± 0.10	-	-
1148.75±0.08	47.3 ± 2.5	24.1± 1.2	318± 20
1157.45±0.09	7.2 ± 0.4	8.6± 0.7	15± 3
1219.40±0.15	1.4 ± 0.1	0.80± 0.20	20± 3
1238.82±0.07	68.0 ± 4.0	71.9± 4.0	74± 5
1277.11±0.07	≡100	≡100	≡100
1286.3 ±0.2	3.75± 0.20	1.9± 0.3	7.2
1308.32±0.08	32.6 ± 1.6	17.0± 1.0	192± 15
1330.50±0.15	0.86± 0.15	0.46± 0.10	-
1340.88±0.09	26.9 ± 1.5	13.0± 0.6	150± 10
1381.4 ±0.3	1.1 ± 0.2	-	16± 3
1401.30±0.08	7.90± 0.40	7.90± 0.40	13± 4
1424.16±0.09	5.75± 0.30	2.2± 0.3	30± 6

Table II
(Continued)

Measured Energies (keV)	Relative Intensities		
	Singles	Anticoincidence	Integral γ-γ Coincidence
1445.80±0.10	2.10± 0.10	2.5± 0.4	-
1479.91±0.10	10.4 ± 0.5	10.4± 0.6	9± 3
1486.20±0.12[d]	1.1 ± 0.1	-	-
1550.5 ±0.4	0.27± 0.04	-	-
1587.6 ±0.5[c,d]	0.15± 0.05	-	-
1617.45±0.15	1.4 ± 0.1	1.6± 0.20	-
1630.9 ±0.6[c,d]	0.14± 0.04	-	-
1639.1 ±0.5	0.20± 0.05	0.55± 0.10	-
1672.02±0.10	1.45± 0.10	1.60± 0.20	-
1678.96±0.13[d]	0.24± 0.03	-	-
1755.32±0.10	0.65± 0.06	0.83± 0.2	-
1813.1 ±0.3[c,d]	0.26± 0.05	-	-

[a] These intensities have been corrected for the underlying peaks from ^{202m}Pb decay using the γ-ray intensities given in Ref. 15.

[b] The γ-γ coincidence experiments indicate that this peak is composed of two transitions of approximately equal intensities.

[c] Assignment to ^{201}Pb uncertain.

[d] Not placed in level scheme.

[e] These energies and intensities have been determined with the aid of the γ-γ coincidence experiment described in §III.D.

Table III

Previously Reported γ Transitions Not Observed in the Present Study

Energy (keV)	*K* Conversion-Electron Intensity[a] (Ref. 12)	Photon Intensity[b] (Ref. 17)	Photon Intensity[b] (Present Study)
58.92±0.05	≈29 (*L*)[c]	--	<15
166.7 ±0.2	1.8 ±0.5	--	< 2.5
225.4 ±0.2	2.3 ±0.8	--	< 1.5
450.39±0.20	--	5.9±1.8	< 1
537.50±0.50	--	2.0±0.9	< 0.3
573.20±0.50	--	6.4±2.3	< 1
602.60±0.20	--	8.9±2.3	< 0.3
760.0 ±0.5	--	≈0.3	< 0.3
760.7 ±0.5	0.46±0.10	--	< 0.3
815.3 ±0.7	0.20±0.05	--	< 0.3
820.3 ±0.5	0.36±0.05	--	< 0.3
969.28±0.20	--	5.0±0.9	< 0.3
1085.30±0.50	--	1.8±0.9	< 0.3
1377.00±0.50	--	3.0±1.4	< 0.3
1420.40±0.50	--	1.1±0.4	< 0.3

[a]The electron intensities of Ref. 12 have been normalized to the photon intensity scale using the *K*-conversion coefficient of the 331-keV transition, 0.113±0.008, measured by Pettersson et al.[11]

[b]Photon intensities are on the same scale as in Table II.

Table III

(Continued)

[c]The 58.92-keV *L*-electron intensity was obtained by subtracting a calculated intensity for the 129.95-keV component from the combined 58.92-keV *L*- and 129.95-keV *K*-electron intensities. The 129.95-keV *K*-electron intensity was calculated by assuming an *M*1 multipolarity and using the theoretical *K*-conversion coefficient[19] along with our measured photon intensity.

Table IV
Results of γ-γ Coincidence Study Using
Two-Parameter Analysis

Gated Energy (keV)	Energies of γ Rays in Coincidence with Gate	
	Strong	Weak
120	826	331,395
124	946,1277	331
130	155,331,598,803	322
155	130,331,803	285
203	331,361,585,946	
232	331,361,406,692,767,1098	309,342
241	331,907	361,546,692, 787,406,1239
285	331,598,804	361,482,692
309	999	232,331
322	331,361,767,826	406,692

Table IV
(Continued)

Gated Energy (keV)	Energies of γ Rays in Coincidence with Gate	
	Strong	Weak
331	130,155,241,285,342,345, 361,381,395,406,465,511, 514,541,546,585,598,638, 709,767,787,804,826,908, 946,999,1063,1070,1089, 1115,1149,1157,1219,1308, 1341,1424	120,232,303, 309,322,728, 753
342	331,361,405,638,692,999	767
345	331,803	
361	322,331,406,465,541,546, 585,598,638,709,728,753, 787,946,1063	232,482,1020
381	331,361,406,692,767,1098	585
395	331,361,585,692,826,946, 1277	907
406	232,331,361,381,541,692	
465	331,361,692	322

Table IV
(Continued)

Gated Energy (keV)	Energies of γ Rays in Coincidence with Gate	
	Strong	Weak
482	331,361,406,826	
511($\gamma^{\pm}$)	331	
514	331,361,465,826	
541	331,361,406,692,767,1098	
546	331,361,692	
585	331,361,395,692	124,309
598	130,331,361,692	285,303
638	331,342,361,692	309
692	309,381,395,406,465,546, 585,638,709,787	241,342,514, 728,753
709	331,361,692	
728	331,361	
753	331,361	
767	232,331,381,541	
787	331,361,692	

Table IV
(Continued)

Gated Energy (keV)	Energies of γ Rays in Coincidence with Gate	
	Strong	Weak
804	130,155,285,331,345	
826	322,331,482,514	
908	241,331	
946	331,361,395,692	322
979		331,692
999	309,331,342	
1063	331,361	
1070	331	
1089	331	
1098	381,541	232
1115	331	
1149	331	
1219		331
1239	241	

Table IV
(Continued)

Gated Energy (keV)	Energies of γ Rays in Coincidence with Gate	
	Strong	Weak
1277	124	395
1308	331	
1341	331	
1381		331
1424	331	

Table V
Internal Conversion Data for ^{201}Pb

Energy (keV)	Photon Intensity	K-Conversion Intensity[a]	Experimental K Conversion Coefficient	Theoretical K Conversion Coefficients[b] M1	Theoretical K Conversion Coefficients[b] E2	Assigned Multipole Order
285.0	10.3± 1.0	7.5± 1.5	0.37 ±0.08	0.38	0.073	M1
308.9	2.3± 0.3	3.0± 0.5	0.67 ±0.15	0.31	1.05(M2)	E1+M21, M1+E2+E01
331.2	4550 ±250	1000	0.113 ±0.008	0.256	0.051	E2+30±4%M1
345.0	18.3± 1.0	7.4± 1.5	0.21 ±0.11	0.23	0.047	M1
361.3	550 ± 30	240 ±10	0.22 ±0.02	0.202	0.042	M1
381.3	12.9± 0.7	4.2± 0.7	0.17 ±0.03	0.175	0.037	M1
394.9	10.8± 0.7	3.6± 1.0	0.17 ±0.05	0.160	0.034	M1
406.0	120 ± 6	33 ± 3	0.14 ±0.02	0.148	0.032	M1
546.3	16.5± 1.0	1.9± 0.2	0.059 ±0.008	0.068	0.017	M1
584.6	211 ± 8	21 ± 2	0.051 ±0.006	0.056	0.015	M1
597.6	19.0± 1.0	0.6± 0.2	0.016 ±0.006	0.053	0.014	E2
692.4	254 ± 12	5.0± 0.5	0.010 ±0.001	0.036	0.010	E2
708.8	46.2± 2.0	4.0± 0.5	0.044 ±0.007	0.034	0.010	M1

Table V
(Continued)

Energy (keV)	Photon Intensity	K-Conversion Intensity[a]	Experimental K Conversion Coefficient	Theoretical K Conversion Coefficients[b] M1	Theoretical K Conversion Coefficients[b] E2	Assigned Multipole Order
753.4	8.8± 0.8	1.5± 0.2	0.087 ±0.016	0.029	0.073(M2)	M2', M1+E2+E01
767.3	194 ± 10	9 ± 1	0.024 ±0.003	0.028	0.0085	M1+20±15%E2
803.7	90 ± 6	1.3± 0.2	0.0074±0.0016	0.025	0.0077	E2
826.3	141 ± 7	2.8± 0.3	0.010 ±0.001	0.023	0.0073	E2+17±6%M1
907.7	362 ± 20	10.7± 1.0	0.015 ±0.002	0.018	0.0061	M1
946.0	452 ± 30	12 ± 1	0.014 ±0.002	0.0164	0.0057	M1
1070.0	72 ± 4	0.8± 0.1	0.0057±0.0010	0.012	0.0045	E2+M1, E2
1098.5	111 ± 6	1.2± 0.2	0.0055±0.0011	0.011	0.0043	E2+18±17%M1
1114.7	9.8± 0.6	0.20± 0.03	0.010 ±0.002	0.011	0.0042	M1
1148.8	47.3± 2.5	0.6± 0.1	0.0065±0.0010	0.010	0.0039	E2+42±17%M1
1238.8	68 ± 4	0.7± 0.1	0.0053±0.0009	0.0083	0.0034	E2+39±19%M1
1308.3	32.6± 1.6	0.6± 0.2	0.0094±0.0040	0.0072	0.0031	M1

[a] Ref. 12.

[b] Ref. 19.

Table VI
$\log ft$ Values for ^{201}Pb Decay as a Function of Decay Energy

Level Energy (keV)	ε-Feeding Intensity	$\log ft$ (Q_ε=1.8 MeV)	$\log ft$ (Q_ε=1.9 MeV)	$\log ft$ (Q_ε=2.0 MeV)
0	≤ 1.4	≥9.4(f_1t)[a]	≥9.5(f_1t)	≥9.6(f_1t)
331	52	6.6	6.7	6.7
692	6.3	7.3	7.4	7.4
1098	6.2	6.8	7.0	7.1
1134	0.5	7.9 [8.0(f_1t)]	8.0 [8.3(f_1t)]	8.1 [8.5(f_1t)]
1157	3.2	7.0	7.2	7.3
1238	7.5	6.6	6.7	6.8
1277	12.5	6.3	6.4	6.6
1290	0.13	8.2 [8.1(f_1t)]	8.4 [8.5(f_1t)]	8.5 [8.7(f_1t)]
1330	1.1	7.2	7.4	7.6
1401	2.4	6.7	6.9	7.1
1420	1.7	6.8	7.0	7.2
1445	0.37	7.4	7.6	7.8
1479	2.8	6.4	6.7	6.9
1550	0.029	8.1 [7.3(f_1t)]	8.5 [8.0(f_1t)]	8.7 [8.5(f_1t)]
1575	≈0.13	≈7.3	≈7.7	≈8.0
1617	0.088	7.2	7.8	8.1
1639	1.5	5.8	6.4	6.8

Table VI
(Continued)

Level Energy (keV)	ε-Feeding Intensity	logft (Q_ε=1.8 MeV)	logft (Q_ε=1.9 MeV)	logft (Q_ε=2.0 MeV)
1672	1.0	5.6	6.4	6.8
1712	0.039	6.5	7.7	8.2 [7.5(f_1t)]
1755	0.18	5.1	6.6	7.3

[a]Log f_1t values were calculated for those ε transitions which are known to be, or could possibly be, first forbidden unique. The other values are, of course, for allowed transitions.

Table VII
β^+-Feeding Intensities for ^{201}Pb Decay

Energy of Level (keV)	Experimental ε Feeding Intensity	Theoretical ε/β^+		Calculated β^+ Feeding		Observed Feeding
		Q_ε=1.8 MeV	Q_ε=2.0 MeV	Q_ε=1.8 MeV	Q_ε=2.0 MeV	
0	≤ 1.4%	1350[a]	512[a]	≤0.0010%	≤0.0027%	
331.15	52%	2270	501	0.023%	0.10%	
692.40	6.3%	9.8×10^6	1.7×10^4	6×10^{-7}%	4×10^{-4}%	
Total				0.024%	0.10%	0.05±0.01%

[a]Calculated for first-forbidden unique β transition.

Table VIII

E2/M1 Multipolarity Mixing Ratios (δ^2)[a] for Transitions in ^{201}Tl

$J_i \rightarrow J_f$[b]	Transition Energy (keV)	δ^2		
		Experiment[c]	Theory (Ref. 1)	Theory (Ref. 2)
$(3/2^+)_1 \rightarrow (1/2^+)_1$	331.15	2.3±0.5	10.0	2.0
$(5/2^+)_1 \rightarrow (3/2^+)_1$	361.25	≈0	0.0032	0.0027
$(3/2^+)_2 \rightarrow (5/2^+)_1$	406.0	≈0	—	—
$(3/2^+)_2 \rightarrow (3/2^+)_1$	767.3	$0.25^{+0.29}_{-0.20}$	—	0.23
$(3/2^+)_2 \rightarrow (1/2^+)_1$	1098.5	$4.6^{+94.4}_{-2.7}$	—	4.5

[a] $\delta^2 \equiv \frac{B(E2)}{B(M1)}$

[b] J_i and J_f are the spins of the initial and final states, respectively. The subscripts 1 and 2 refer to the first and second levels (increasing energy) of a given spin.

[c] The experimental values of δ^2 were obtained from our measured *K*-conversion coefficients, Table V, and the theoretical conversion coefficients of Hager and Seltzer.[19]

Table IX

γ-Ray Branching Ratios from States in ^{201}Tl

State Energy (keV)	Transition Energies (keV)	$\frac{J_i \rightarrow J_f}{J_i \rightarrow J_f'}$	γ-Ray Branching Ratio		
			Experiment	Theory (Ref. 1)	Theory (Ref. 2)
692.40	$\frac{361.25}{692.4}$	$\frac{(5/2^+)_1 \rightarrow (3/2^+)_1}{(5/2^+)_1 \rightarrow (1/2^+)_1}$	2.2 ±2	1.6	2.5
1098.4	$\frac{406.0}{1098.5}$	$\frac{(3/2^+)_2 \rightarrow (5/2^+)_1}{(3/2^+)_2 \rightarrow (1/2^+)_1}$	1.08±8	—	0.95
	$\frac{767.3}{1098.5}$	$\frac{(3/2^+)_2 \rightarrow (3/2^+)_1}{(3/2^+)_2 \rightarrow (1/2^+)_1}$	1.75±0.13	—	1.85
1134.8	$\frac{442}{803.7}$	$\frac{(7/2^+)_1 \rightarrow (5/2^+)_1}{(7/2^+)_1 \rightarrow (3/2^+)_1}$	<0.011[a]	0.0091	0.01
1290.0	$\frac{155.3}{597.6}$	$\frac{(9/2^+)_1 \rightarrow (7/2^+)_1}{(9/2^+)_1 \rightarrow (5/2^+)_1}$	0.43±6	—	0.29

[a] The 442-keV transition was not observed in this study, so the branching ratio is based on our upper limit for its intensity.

FIGURE CAPTIONS

Figure 1 ^{201}Pb singles γ-ray spectrum recorded by a 3.6%-efficient Ge(Li) detector during a 24-h period. The ^{201}Pb source was prepared by the $(p,3n)$ reaction on a 70%-enriched ^{203}Tl target.

Figure 2 ^{201}Pb anticoincidence γ-ray spectrum taken with a 2.5%-efficient Ge(Li) detector placed inside a 20.3×20.3-cm NaI(Tl) split annulus with a 7.6×7.6-cm NaI(Tl) detector blocking the other end. Only peaks belonging to ^{201}Pb decay are labeled except where indicated.

Figure 3 ^{201}Pb integral coincidence γ-ray spectrum taken with 2.5% and 3.6% Ge(Li) detectors. All γ rays above the Tl *K* x-rays were included in the gate.

Figure 4 Several examples of gated coincidence spectra obtained from the two-parameter γ-γ megachannel coincidence experiments on ^{201}Pb. These gated spectra have had the background subtracted and were obtained by gating on signals from the 3.6% Ge(Li) detector and displaying those from the 2.5% detector.

Figure 5 Results from the two-parameter γ-γ coincidence experiment used to determine the energies of the γ rays in the 945.96- and 946.78-keV doublet. A) *Y*-side integral coincidence spectrum used for the gates. The γ rays which have (946) after the energies were in coincidence with only the lower-energy member of the doublet; those with (947), with only the higher-energy member. B) *X*-side integral coincidence spectrum showing the region near the doublet on an expanded scale. C) Sum of the gated coincidence spectra showing the 945.96-keV peak. D) Sum of the gated coincidence spectra showing the 946.78-keV peak.

Figure 6 Experimental vs. calculated *K*-shell conversion coefficients for transitions following the decay of ^{201}Pb. The smooth curves were drawn to fit the calculated values of Hager and Seltzer.[19]

Figure 7 ^{201}Pb decay scheme. Energies are given in keV and (total) transition intensities in per cent of ^{201}Pb disintegrations. The per cent ε decay and corresponding log*ft* value are listed to the right of the levels. The log*ft*'s are based on Q_ε = 1.9 MeV. (*There are two ≈285.0-keV γ transitions.)

Figure 8 Systematics of states below 1.8 MeV in neutron-deficient odd-mass Tl isotopes as observed in radioactive decay and particle-transfer reaction studies. The states of ^{207}Tl are from Ref. 35; those of ^{203}Tl and ^{205}Tl, from Refs. 36-40; those of ^{201}Tl, from the present work except for the $(9/2^-)$ state, which is from Ref. 41; those of ^{199}Tl, from Refs. 18 and 33; and those of ^{197}Tl, ^{195}Tl, and ^{193}Tl, from Refs. 42 and 43. The J^π's given for ^{201}Pb states in this figure are the most probable assignments and differ from those shown in Fig. 7 in that we have omitted some of the less likely assignments for the sake of clarity.

Figure 9 A comparison of the experimental states (A) in ^{201}Tl with the weak-coupling calculations of Covello and Sartoris (B) and Alaga and Ialongo (C).

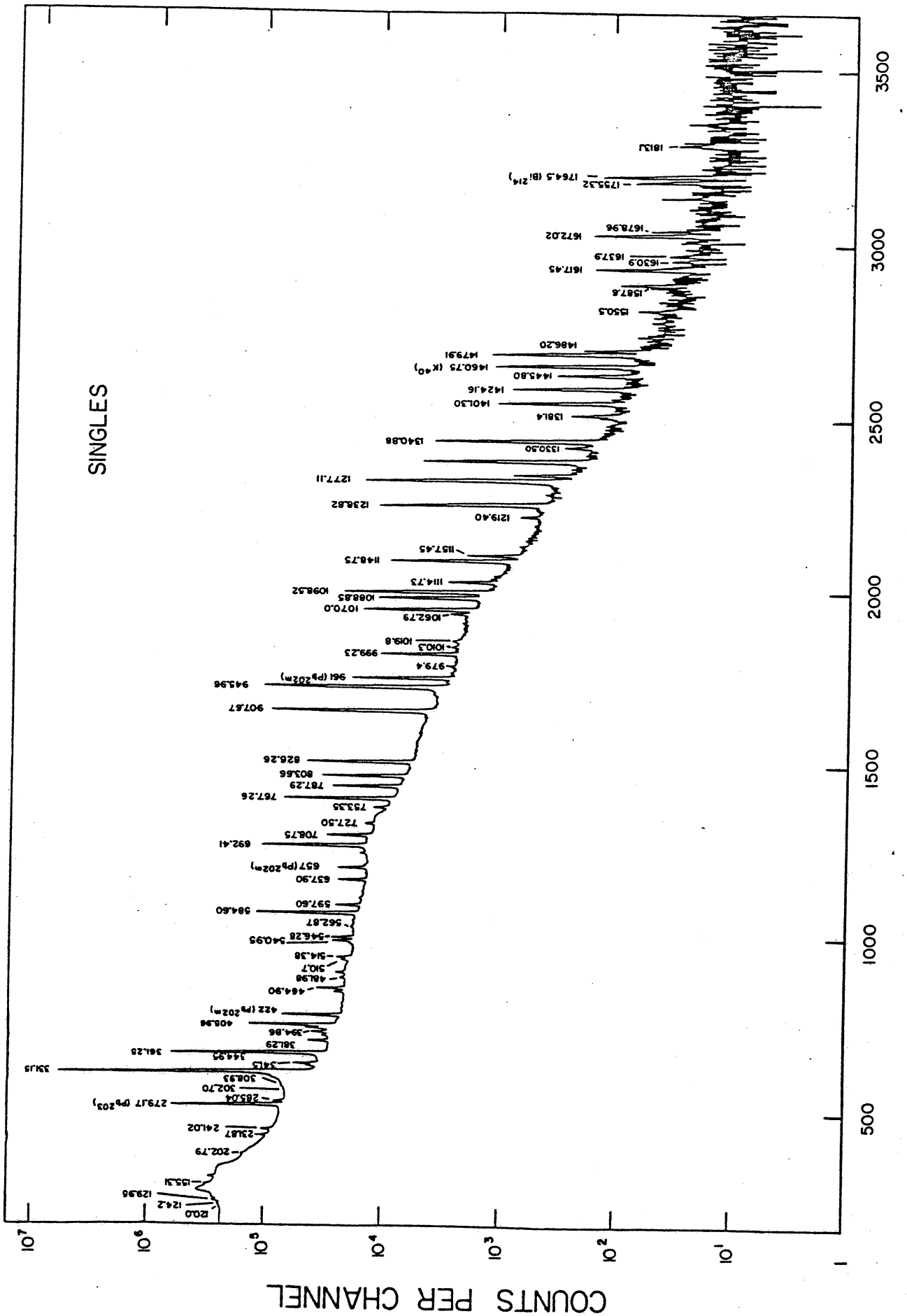
SINGLES
COUNTS PER CHANNEL
CHANNEL NUMBER
500
1000
1500
2000
2500
3000
3500
10^{7}
10^{6}
10^{5}
10^{4}
10^{3}
10^{2}
10^{1}
1
R00
1242
1293.6
153.31
202.79
238.7
241.02
279.17 (Pb^{203})
285.04
302.70
308.33
346.5
331.15
361.25
381.29
394.86
408.96
422 (Pb^{202m})
464.90
481.98
510.7
514.38
546.28
540.93
562.87
584.60
597.60
637 (Pb^{202m})
637.90
692.41
708.75
727.50
753.35
767.26
787.29
803.66
826.26
907.87
943.96
961 (Pb^{202m})
979.4
999.23
1010.3
1019.8
1062.79
1070.0
1088.85
1098.52
1114.73
1148.75
1157.45
1219.40
1238.82
1277.11
1330.50
1340.88
1381.4
1401.30
1424.16
1445.80
1460.75 (K^{40})
1479.91
1486.20
1550.5
1587.8
1617.45
1630.9
1637.9
1672.02
1678.96
1755.32
1764.5 (Bi^{214})
1813.1

Figure 1

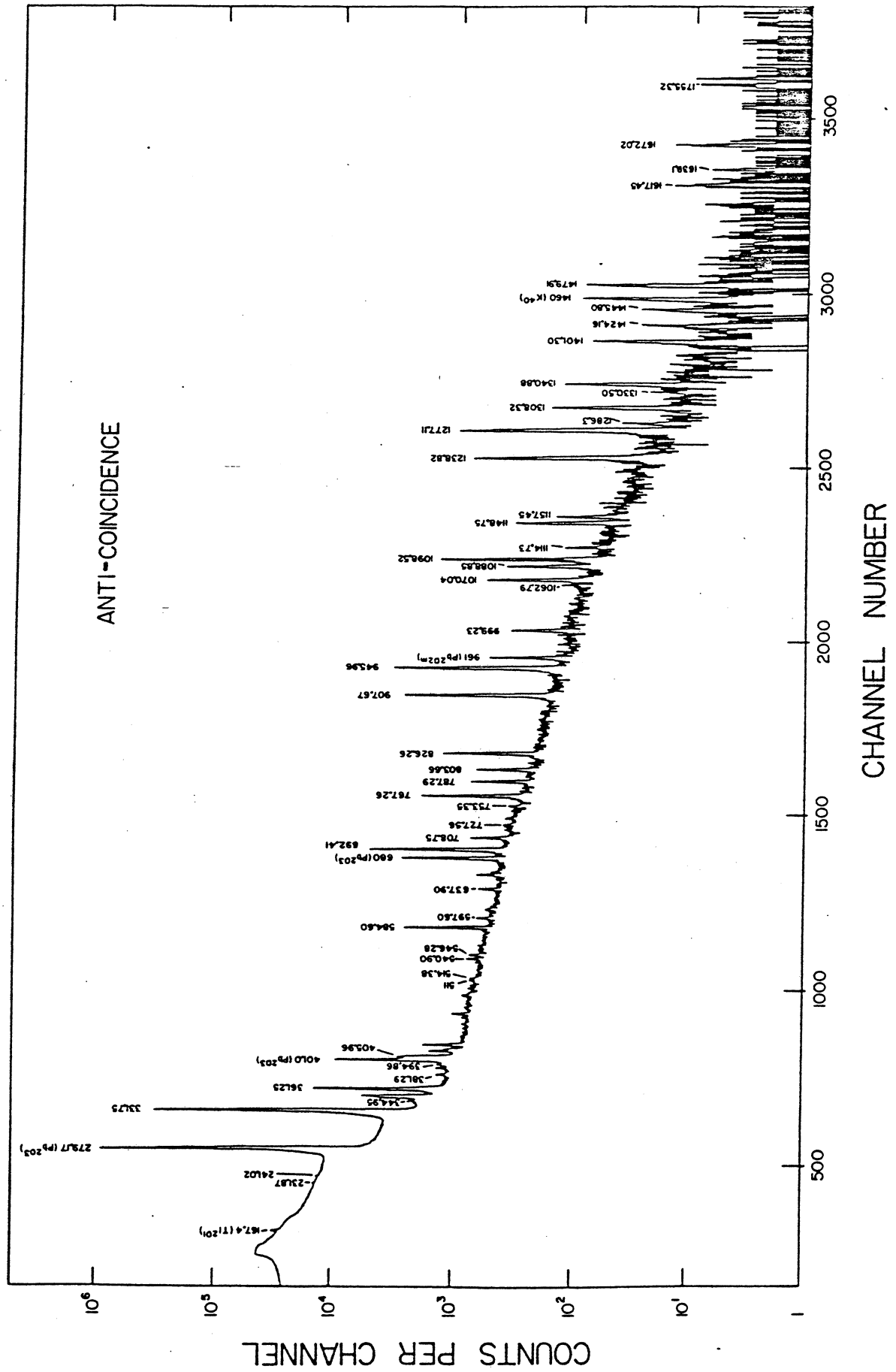
ANTI-COINCIDENCE
COUNTS PER CHANNEL
CHANNEL NUMBER
500
1000
1500
2000
2500
3000
3500
10^6
10^5
10^4
10^3
10^2
10^1
1
467.4 (Tl^{208})
2386.7 (Pb^{203})
2614.02
3332.73
3614.23
4040 (Pb^{203})
4053.96
680 (Pb^{203})
692.41
961 (Pb^{202m})
1062.79
1088.83
1098.52
1157.45
1238.82
1277.11
1340.88
1401.50
1460 (K^{40})
1672.02
1753.32

Figure 2

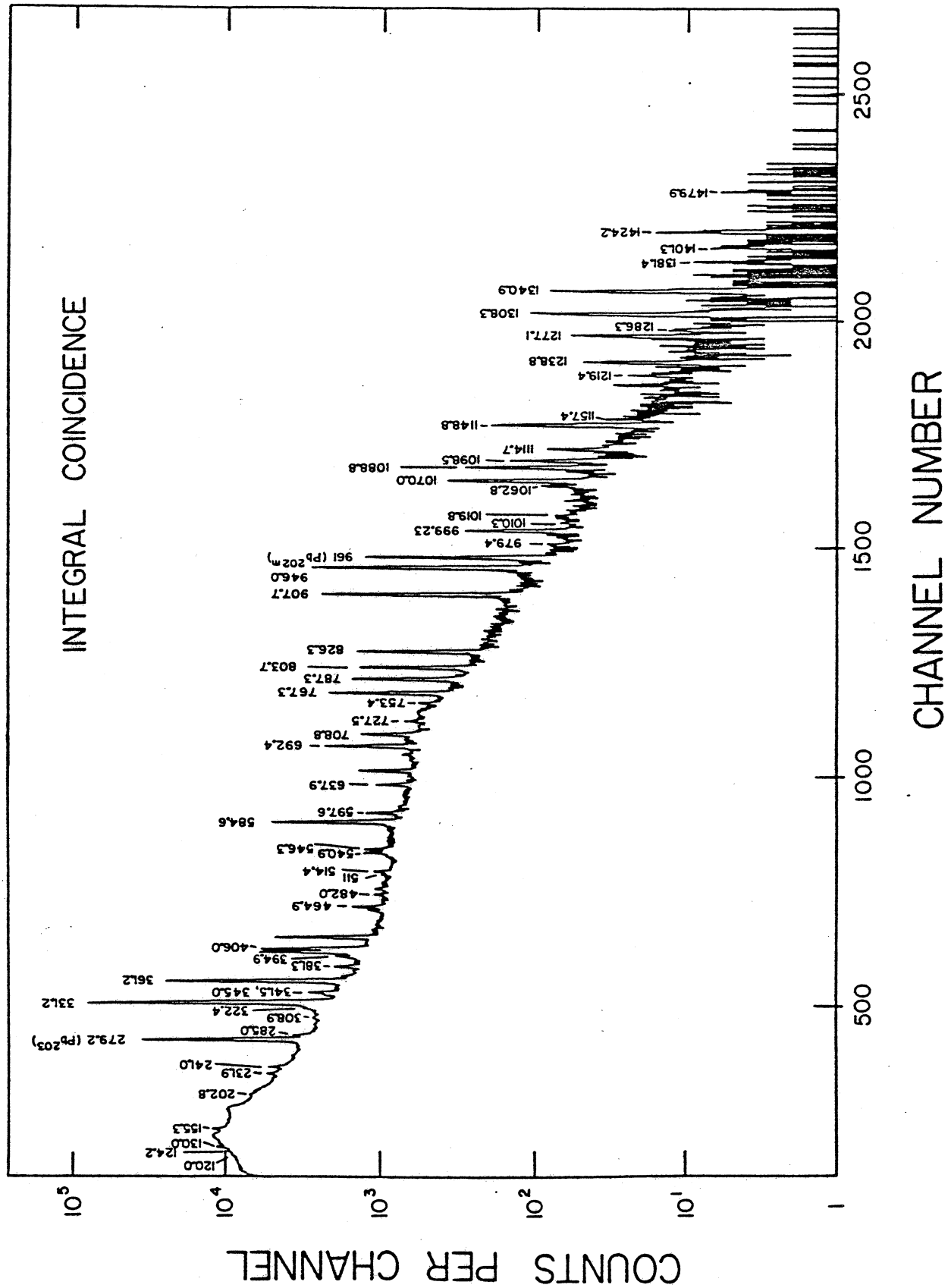
INTEGRAL COINCIDENCE
COUNTS PER CHANNEL
CHANNEL NUMBER
500
1000
1500
2000
2500
1200
1242
1300
1553
2028
2319
2410
2792 (Pb203)
2830
3082
3224
3415, 3450
3312
3612
3813
3949
4060
4649
4820
5111
5144
5409
5463
5846
5976
6379
6925
7087
7273
7534
7673
7873
8033
8263
9070
9460
961 (Pb202m)
9794
9993
10103
10198
10628
10700
10865
10888
11147
11484
11574
12194
12388
12771
12863
13083
13409
13814
14051
14242
14799

Figure 3

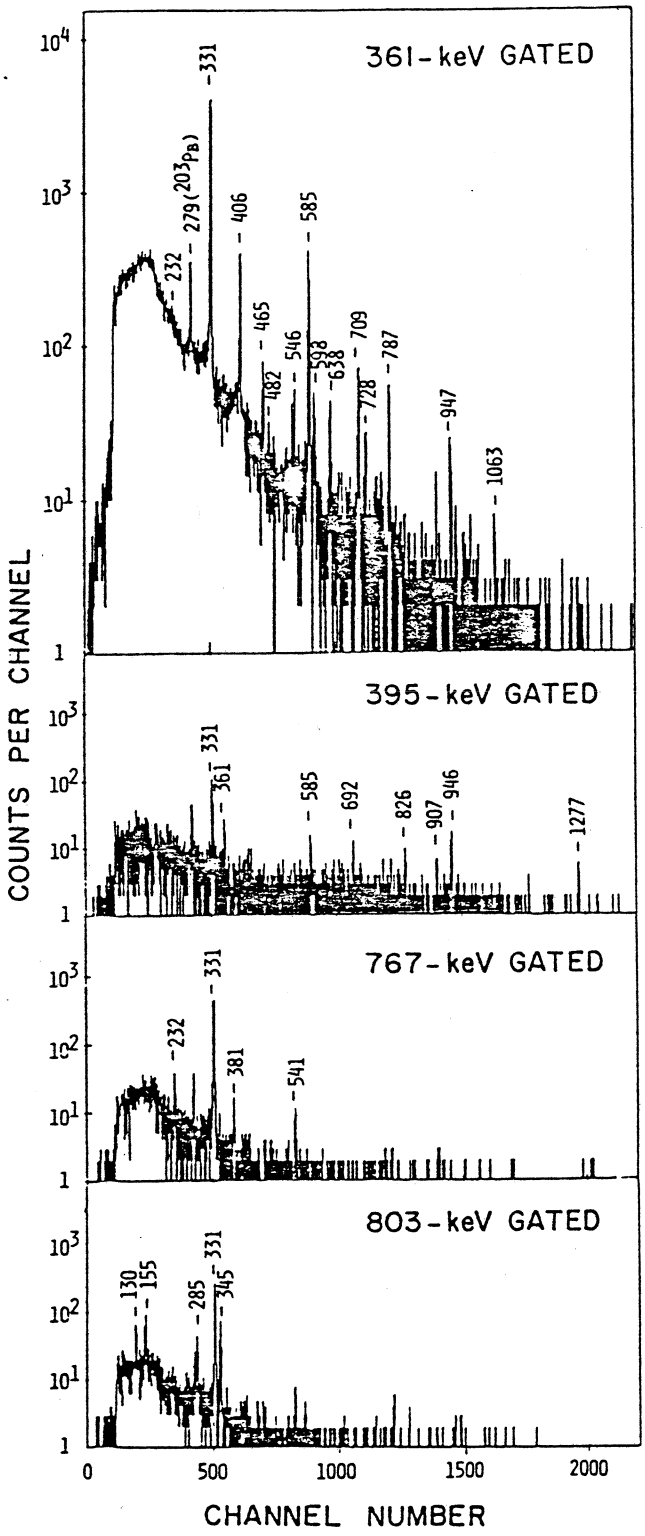
361-keV GATED
395-keV GATED
767-keV GATED
803-keV GATED
COUNTS PER CHANNEL
CHANNEL NUMBER
331
279(203Pb)
232
406
585
465
546
482
598
638
709
728
787
947
1063
361
692
826
907
946
1277
381
541
130
155
285
345
0
500
1000
1500
2000

Figure 4

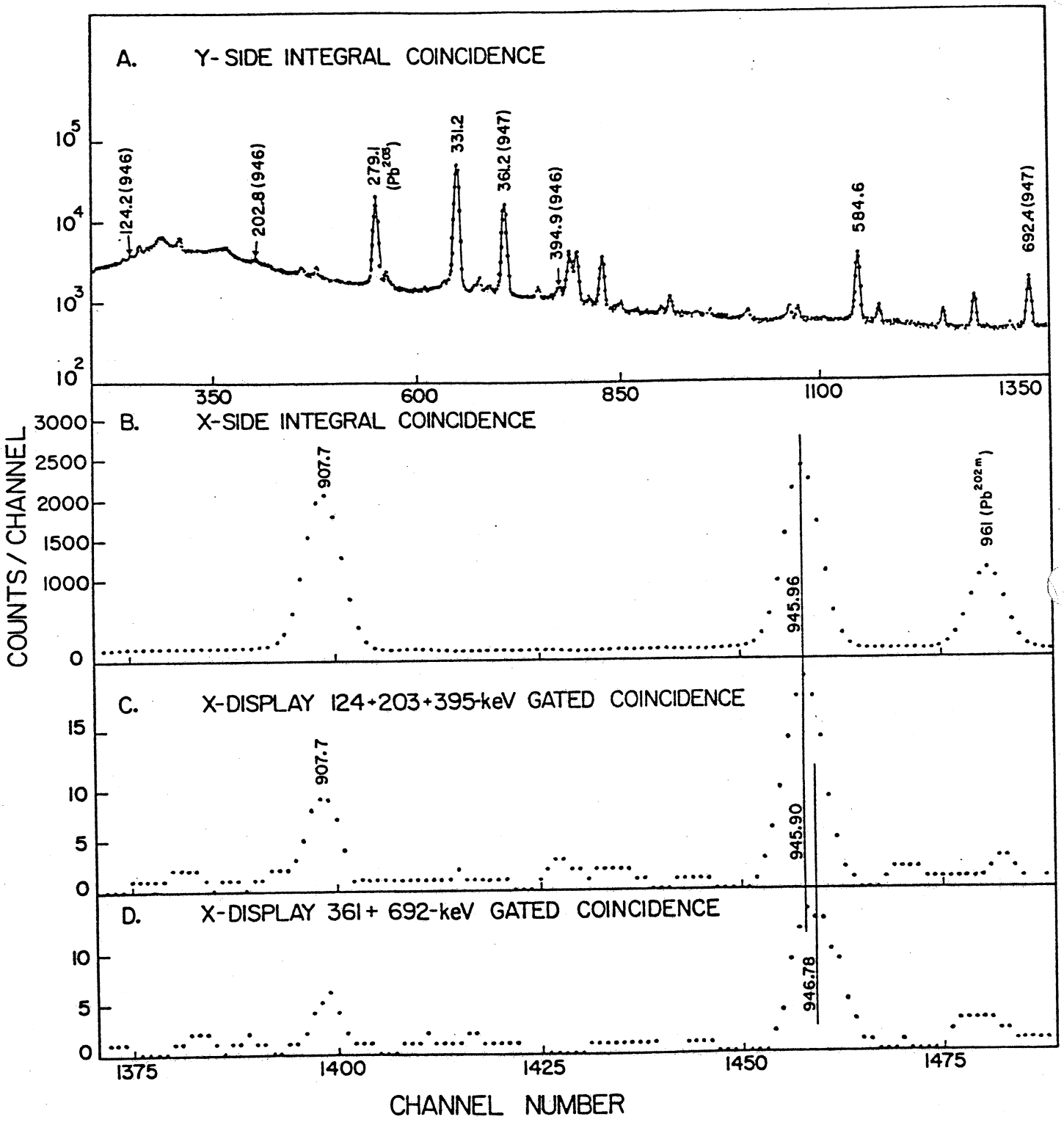
A. Y-SIDE INTEGRAL COINCIDENCE
124.2(946)
202.8(946)
279.1 (Pb208)
331.2
361.2(947)
394.9(946)
584.6
692.4(947)
B. X-SIDE INTEGRAL COINCIDENCE
907.7
945.96
961 (Pb202m)
C. X-DISPLAY 124+203+395-keV GATED COINCIDENCE
907.7
945.90
D. X-DISPLAY 361+ 692-keV GATED COINCIDENCE
946.78
COUNTS / CHANNEL
CHANNEL NUMBER

Figure 5

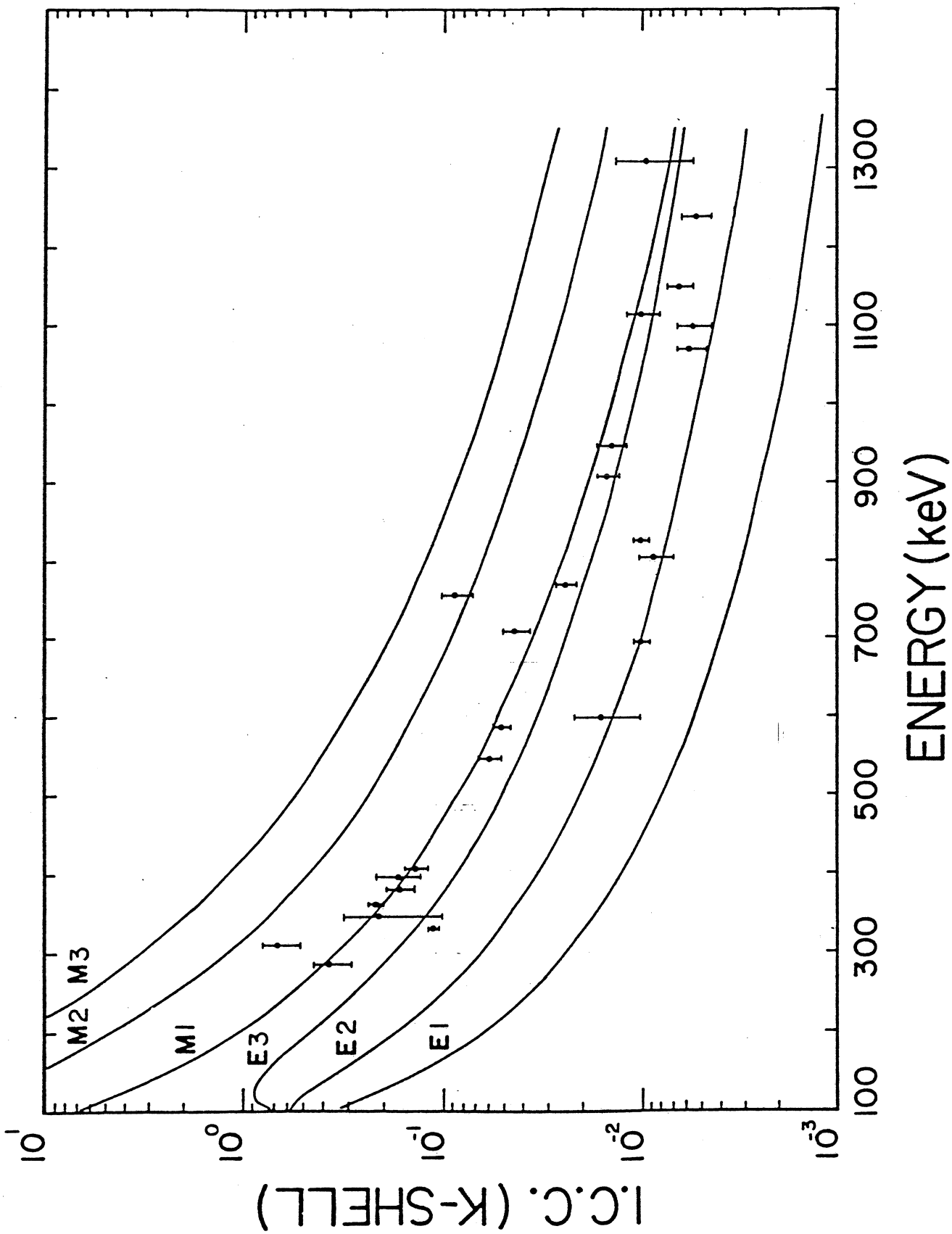
I.C.C. (K-SHELL)
ENERGY (keV)
M3
M2
M1
E3
E2
E1
10^{-1}
10^{0}
10^{-1}
10^{-2}
10^{-3}
100
300
500
700
900
1100
1300

Figure 6

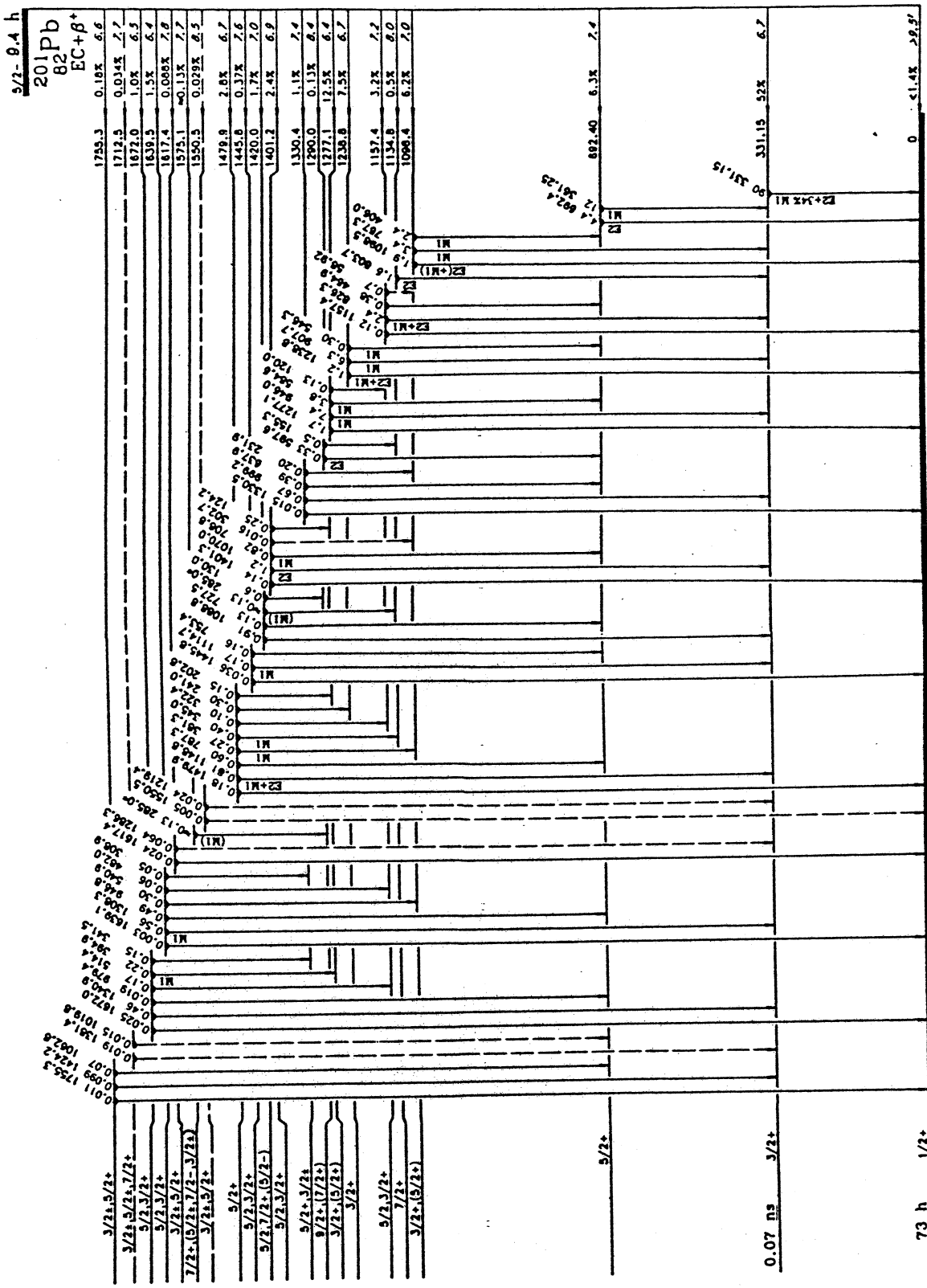

Figure 7

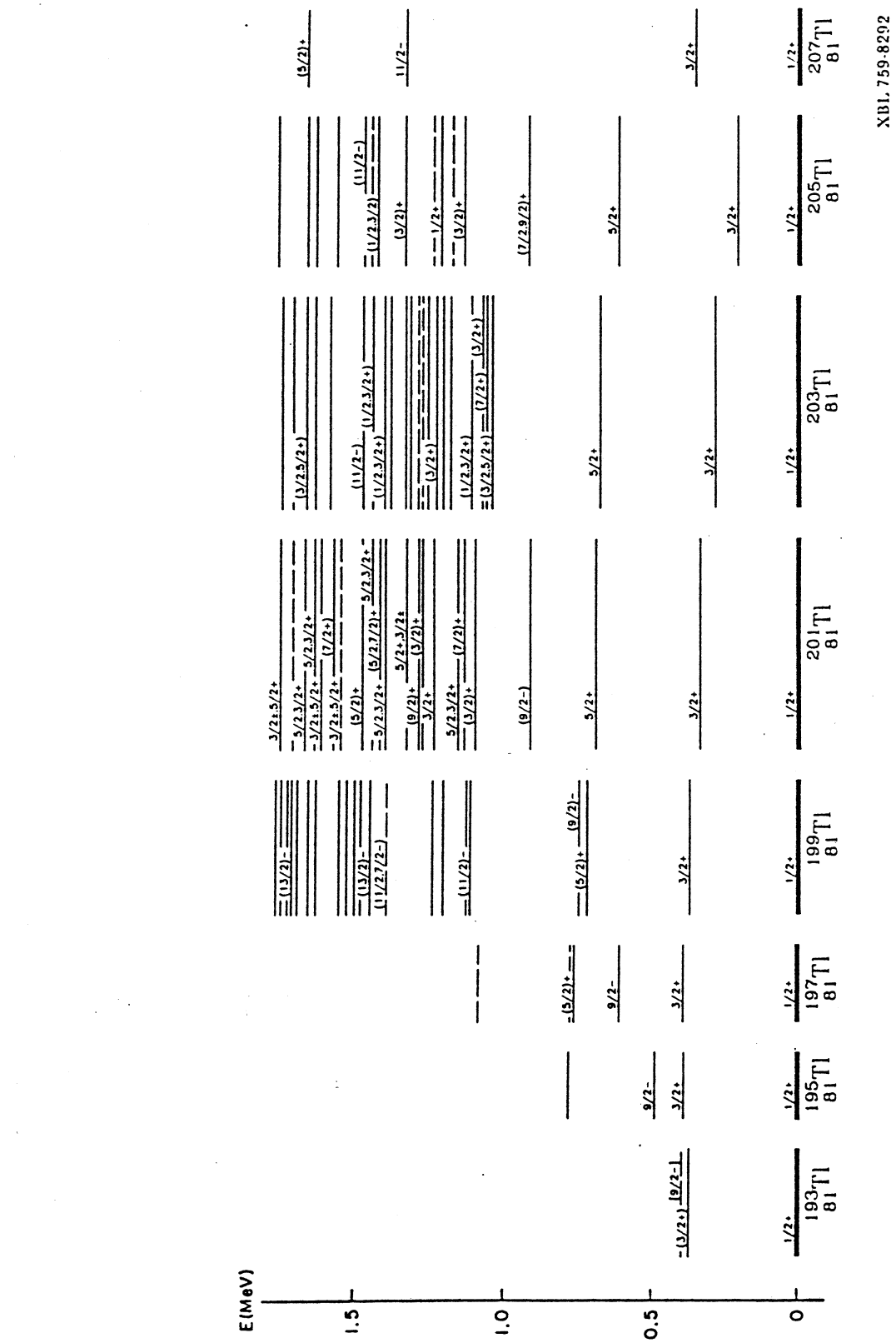
E(MeV)
1.5
1.0
0.5
0
1/2+
193 81 Tl
1/2+
195 81 Tl
1/2+
197 81 Tl
1/2+
199 81 Tl
1/2+
201 81 Tl
1/2+
203 81 Tl
1/2+
205 81 Tl
1/2+
207 81 Tl
XBL 759-8292

Figure 8

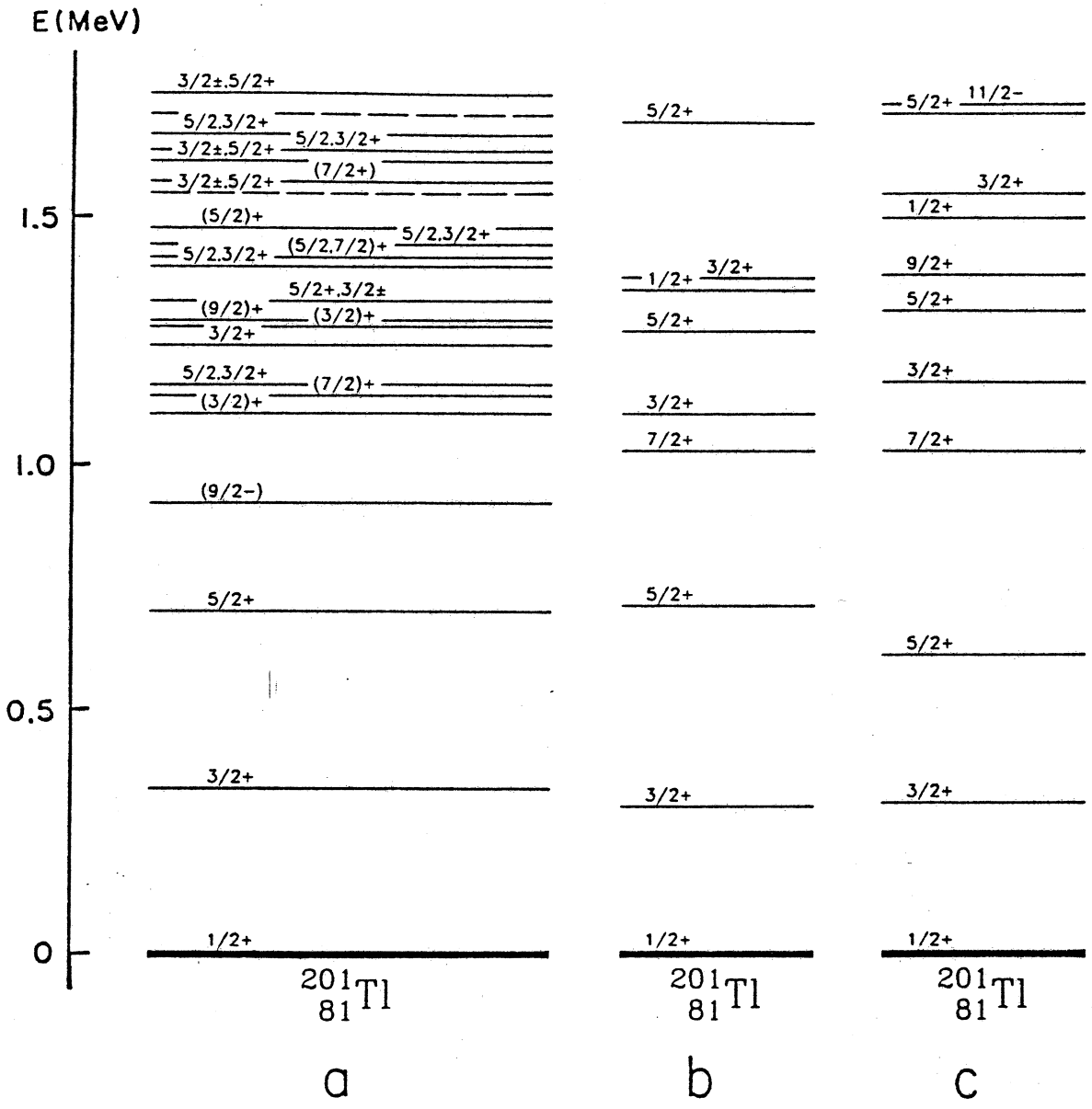
E(MeV)
1.5
1.0
0.5
0
3/2±,5/2+
5/2,3/2+
3/2±,5/2+
5/2,3/2+
3/2±,5/2+
(7/2+)
(5/2)+
5/2,3/2+
5/2,3/2+
(5/2,7/2)+
5/2+,3/2±
(9/2)+
(3/2)+
3/2+
5/2,3/2+
(7/2)+
(3/2)+
(9/2-)
5/2+
3/2+
1/2+
201 81 Tl
a
5/2+
1/2+
3/2+
5/2+
3/2+
7/2+
5/2+
3/2+
1/2+
201 81 Tl
b
5/2+
11/2-
3/2+
1/2+
9/2+
5/2+
3/2+
7/2+
5/2+
3/2+
1/2+
201 81 Tl
c

Figure 9